CHAPTER 7

Glasses and Amorphous Material

7.1 Introduction

In the previous chapters our attention has been focused on materials that achieve their physical characteristics through order in the solid state. Another very important class of materials are those that produce solids which are characterized by a complete lack of order: these are the glasses. Window glass is the amorphous form of SiO_2 which also occurs as a variety of naturally occurring crystalline minerals: quartz, feldspar micas, amphiboles and pyroxens. Glasses are formed from B_2O_3, P_2O_5, As_2S_3, *etc*. Some small molecules form glasses, such as phenyl ethers, 2-methylpentane and glycerine, as do a number of polymers, such as poly(methyl methacrylate) (PMMA) and polystyrene:

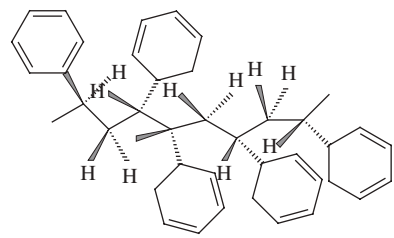

The carbon atom next to the phenyl is potentially a chiral centre, and polystyrene produced by the usual method of radical-initiated polymerization produces an atactic polymer that does not form an ordered solid. However, the use of an ionic route can produce an isotactic form which can lead to a crystalline form of the polymer.[1] The polymer is able to form a helical structure that can pack to form a crystalline solid.

It will be evident that whilst polymers are able to form glasses they are not unique and that the basic characteristics of the glassy state are common to a number of organic and inorganic materials. Some materials, such as *ortho*-terphenyl, form a glass if cooled quickly and subsequently change to a crystalline form.[2]

7.2 Phenomenology of the Glass Transition

The common characteristic exhibited by all glass-forming solids is a similarity in their thermal expansion behaviour. Most crystalline solids exhibit a linear expansion coefficient up to their melting point, whereupon they undergo a discontinuous increase in volume over a small temperature range. Glasses, in contrast, exhibit at very low temperatures a linear expansion coefficient similar to that of a crystalline solid, but at some temperature there is a change in the slope of the expansion coefficient marking the solid taking on a deformable characteristic. The X-ray scattering from glassy solids is usually rather broad and indicates that there is present in the solid a broad spectrum of scattering lengths and usually no clear indication of a primary unit cell structure. High molar mass polymeric materials have the added characteristics of forming a rubbery state which gives the transition from solid to rubber its name: T_g, glass to rubber transition. One of the simplest methods of determining T_g is to measure the change in volume of a polymer with temperature using a dilatometer.[3] The typical plot for a crystallizable glass-forming material such as *o*-terphenyl (Figure 7.1a) shows certain characteristic features. Fast cooling of the melt allows supercooling to a glass that may or may not be stable. At T_g the temperature dependence becomes parallel to that of the crystalline form. In the case of *o*-terphenyl the crystalline form is created after storing the glass close to its T_g value for a long time. On heating the crystalline form the expansion follows that of a classic ordered material showing an abrupt change in volume at the melt temperature.

A further facet of glass-forming solids is that the volume of the glassy state depends on the cooling rate (Figure 7.1b). Rapid cooling creates a solid with a higher apparent volume than if the material is slowly cooled. The inflection point depends on the rate of the cooling of the material, indicating that the value of T_g, unlike T_m, is not a fixed quantity and indicates that this transition is defining a metastable state of matter. Despite the apparent flexibility of the

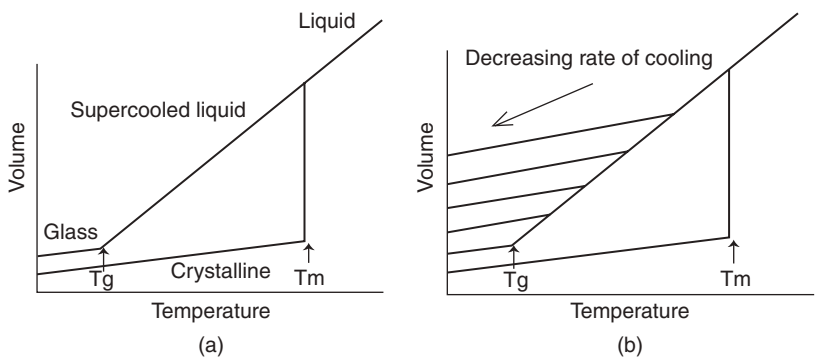

Figure 7.1 Schematic of the variation in the volume with temperature of glassy and crystalline *ortho*-terphenyl: (a) cooling–heating; (b) variation with cooling rate.

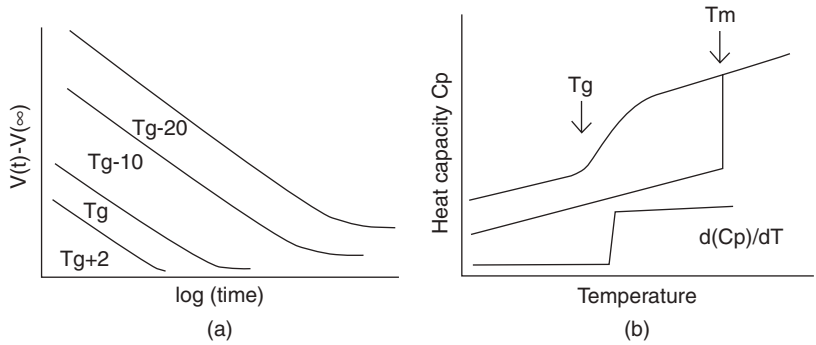

Figure 7.2 (a) Variation of the isothermal volume contraction. V(t) is the volume at time t minus the infinite volume of the solid, crystalline, value as a function of log(time). (b) Variation of the heat capacity C_p and its derivative in the region of T_m and T_g.

T_g value, it is a fairly well-behaved property that has been very well studied and is now fairly well understood.[5] Storage of the glass below T_g allows observation of the variation of the volume with time (Figure 7.2). The exact temperature dependence can change slightly with the form of the glass but most materials exhibit a variation that is approximately logarithmic with time.

The glass undergoes densification on ageing and this process is the basis of *physical ageing*, a phenomenon that has been extensively investigated by Stuick.[5]

An alternative and popular method of studying the glass–rubber transition is through differential scanning calorimetry[3] and the measurement of the heat capacity, C_p. For a crystalline solid the heat capacity will exhibit a discontinuous change at the melting point T_m, and this is designated a *first*-order phase transition (Figure 7.2b). In contrast, the first derivative of the heat capacity undergoes a discontinuous change at T_g and this is therefore designated a *second*-order transition. Since enthalpy exhibits phenomena very similar to those of the volume, it is not surprising that time-dependent *relaxation* processes are observed when the samples are stored below T_g. The relaxation of the enthalpy or the volume is termed *physical ageing*.[5]

7.2.1 Dynamic Mechanical Thermal Analysis

Another characteristics feature of the glass transition is the associated change in the modulus. The stress, *elongation*, is related to the strain, the force applied to a material by the *modulus*. Conventionally there are two approaches to the measurement of the modulus: static and dynamic. The static method involves measurement of the stress–strain profile and from the slope of the curve the elastic modulus can be determined. The dynamic method subjects the sample to a periodic oscillation and explores the variation of the amplitude and phase of the response of the sample as a function of temperature. A small sample of the test material is subjected to displacement as shown in Figure 7.3.

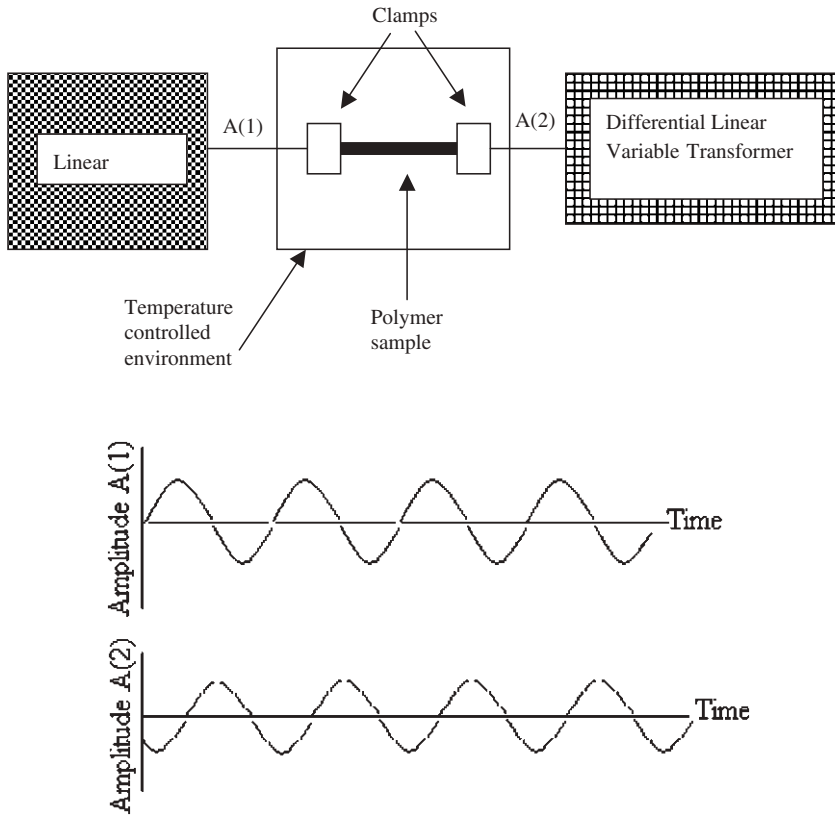

Figure 7.3 Schematic diagram of the dynamic mechanical thermal analysis experiment (top) and a comparison of the amplitudes of the oscillation at points (1) and (2) for a semi-flexible material (bottom).

The oscillation is provided by a linear motor that is able to provide a constant phase and amplitude that is independent of temperature and the forces that are applied to the sample. The variation of the amplitude at point (1) is designated $A(1)$ and that at point (2) is designated $A(2)$. Depending on the stiffness of the material, the amplitude $A(2)$ will vary with temperature and also the frequency of the oscillation. The amplitude $A(1)$ represents the stress which is applied to the sample and $A(2)$ is the corresponding strain that is generated. The stress and the strain are related through the complex modulus E^*; the shift along the time axis of the oscillations is the phase angle ϕ. For a rigid material the phase angle will be approximately zero. As the material softens the phase angle will increase reaching a maximum value at T_g. Softening of the material will increase the difference in the amplitudes until in the limit $A(2)$ would tend to zero as the material becomes infinitely flexible. Comparison of complex functions is best carried out using an Argand diagram in which the stress (σ) and strain (ε) are represented as complex quantities and resolved into real and

imaginary components. The σ vector can be resolved into two components: σ' in phase and σ'' out of phase with ε. Two moduli can be defined, G' and G'' representing the in- and out-of-phase components of the complex modulus G^*. The in-phase modulus is defined as $G' = \sigma'/\varepsilon$ and the out-of-phase components as $G'' = \sigma''/\varepsilon$. Since $\sigma' = \sigma \cos \delta$ and $\sigma'' = \sin \delta$, then $G' = \sigma'/\varepsilon = (\sigma \cos \delta)$, and similarly $G'' = G^* \sin \delta$. Using the notation of complex numbers, $\sigma = \sigma' + i\sigma''$ since σ is the vector sum of σ' and σ''. Thus $G^* = \sigma/\varepsilon = (\sigma' + i\sigma)/\varepsilon = G' + iG''$. The ratio $G''/G' = \tan \delta$ is referred to as the *loss factor*. The out-of-phase or loss modulus represents the energy that is not recovered on deformation and is dissipated as heat. If we take a rubber band and subject it to rapid oscillation it will heat up and this is a measure of the energy that has been supplied to the molecules in the form of elongation of the chains that is not recovered when the force is removed. The loss modulus is obtained from the phase information obtained from the dynamic measurements and tells us directly about the ability of the polymer chains in the material to move. The technique and analysis of data are described elsewhere.[4,6]

Most glassy polymers will exhibit a modulus at low temperature which is of the order of 10^{10}–10^9 Pa. At the glass transition the modulus will have dropped to a value of the order of 10^6 Pa and the material will now have rubbery characteristics. This drop in modulus is accompanied by an increase in the loss modulus that will peak at T_g as shown in Figure 7.4.

7.2.2 Dielectric Relaxation Spectroscopy (DRS)

A number of studies have been carried out of the glass transition process using dielectric relaxation spectroscopy. With the advent of computer-assisted measurements[7] the DRS technique has increased in popularity and is now routinely used for the study of molecular mobility in polymeric materials. Chemical bonds may possess dipole moments as a consequence of the differences in

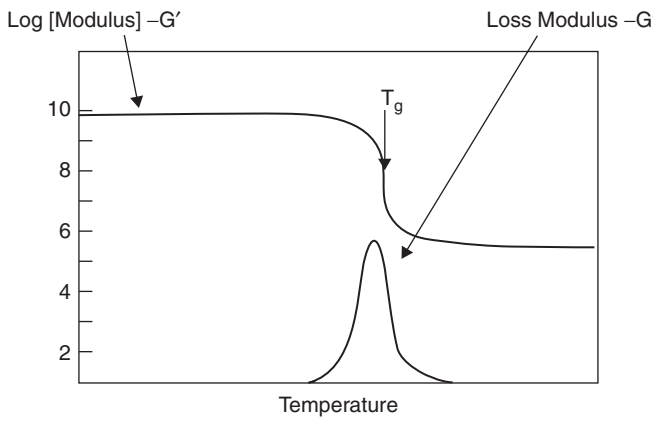

Figure 7.4 Schematic of a dynamic mechanical thermal analysis plot of a glass-forming polymer.

electron density between the atoms forming the chemical bonds. However, whether or not a polymer has a net dipole moment will depend on the symmetry of the polymer and whether the vectorial components of the dipoles are able to cancel. A polymer such as polytetrafluoroethylene has a high degree of regularity and symmetry and consequently a very small dipole moment despite the bond dipole being high. If a molecule is placed in an electric field the molecule will attempt to move to achieve a minimum energy situation that corresponds to the dipole being aligned with the field. If the field instead of being static is allowed to oscillate the ability of the dipoles to follow the applied field depends on their intrinsic mobility. A characteristic frequency exists at which the frequency of oscillation and the natural relaxation will be equal. This is the so-called *relaxation frequency*. The dependence of the electronic polarizability (α) on the frequency of oscillation (ω) depends on physical characteristics of the system. An electric field induces a distortion of the electronic clouds associated with the chemical bonds and is responsible for the refractive index (n) of the material measured at optical frequencies, 10^{15} Hz, and is designated the *electronic polarization* (Figure 7.5). According to the Clausius–Mossotti equation:

$$\frac{n^2 - 1}{n^2 + 2} = \frac{4\pi\rho N_A}{3M}\alpha_e \tag{7.1}$$

where N_A is Avogadro's number, M is the molar mass and ρ is the density. On lowering the frequency into the optical–infrared region (10^{13} Hz) additional contributions are observed which correspond to the vibrations, rocking and twisting motions that are characteristic of the molecule.

These are resonant processes and conventional infrared spectroscopy investigates the dielectric loss processes associated with these resonances and are designated *atomic polarization* and *bond polarization*. In Figure 7.5 the vertical lines denote the resonance features that are characteristics of a particular molecular structure and occur in the infrared. These resonances are used by

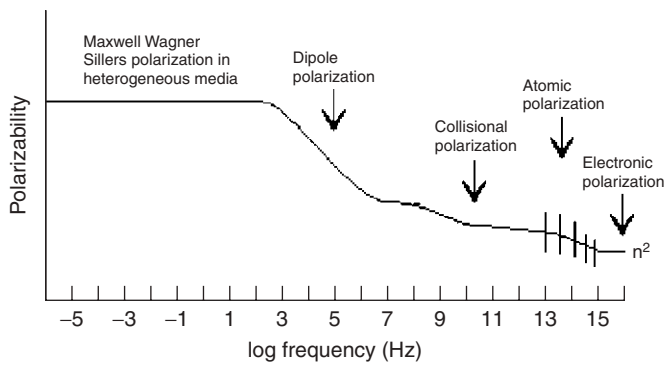

Figure 7.5 Schematic of the frequency dependence of the polarizability as a function of frequency for a polar system.

chemists to identify the nature of the molecular structure. At lower frequencies, molecules can exhibit an additional polarization that is due to the distortions in the electron cloud when molecules undergo inelastic collisions and energy is transferred into excited vibrational states. This contribution is designated *collision polarization*. However the main contribution to the polarizability arises from the alignment of the permanent dipoles and their motion is controlled by the local force field in which they find themselves. In the case of a small molecule, the viscosity of the fluid determines the rate at which the dipole can align. In the case of a polymer solid, the rate of alignment depends on how rigidly the dipole is attached to the polymer chains. The relaxation process can occur anywhere in the accessible frequency range that is currently between 10^{-5} Hz and 10^{11} Hz.

The dielectric relaxation experiment can be visualized in terms of a simple capacitor in which the dipoles are aligned by an applied electric field (E). The magnitude of the charge–displacement field that is observed on the plates depends on the polarizability of the media between the plates of the capacitor. The greater the polarizability the larger the charge that can be carried by the plates. The polarization (P) induced per unit volume for a material placed between parallel plates in a capacitor can be related to the susceptibility χ of the material to be polarized:

$$P = \chi \varepsilon_0 E \tag{7.2}$$

where ε_0 is the permittivity of free space. The capacitance (C) of the capacitor is defined as the amount of charge it can store per unit voltage and the dielectric permittivity is defined by

$$\varepsilon = \frac{C}{C_0} \tag{7.3}$$

where C_0 is the capacitance when the capacitor is in vacuum. The dielectric permittivity ε is defined as

$$\varepsilon = (1 + \chi) \tag{7.4}$$

Combining eqn (7.2) with eqn (7.4) gives

$$P = (1 + \chi)\varepsilon_0 E = \varepsilon \varepsilon_0 E \tag{7.5}$$

In a simple experiment removal of the applied field allows the polarization in the capacitor to decay as a consequence of the randomization of the dipoles. The decay will be determined by a *relaxation time* τ. The decay of the polarization in the capacitor can be described by

$$P(t) = P_0 \exp\left(-\frac{t}{\tau}\right) \tag{7.6}$$

As in the case of the dynamic mechanical experiment we are dealing with mathematical complex quantities. The dielectric permittivity should be

expressed as a complex quantity ε^*:

$$\varepsilon^* = \varepsilon' - \mathrm{i}\varepsilon'' \tag{7.7}$$

where ε' is the dielectric permittivity and ε'' is the dielectric loss. Normally experiments are performed in the frequency rather than the time domain.[6,7] The time domain can be transformed into the frequency domain using the Laplace transform:

$$P^*(\omega) = L\left(-\frac{\partial[P(t)]}{\partial t}\right) \tag{7.8}$$

The angular frequency ω dependence of the complex permittivity can be described by

$$\varepsilon^* = \varepsilon_\infty + \frac{(\varepsilon_0 - \varepsilon_\infty)}{(1 + \mathrm{i}\omega\tau)} \tag{7.9}$$

where ε_∞ is the high-frequency limiting value of the of the permittivity and ε_0 is the low-frequency limiting value or static polarizability. In practice, this formulation is only used to describe dipolar processes and an alternative approach is used to describe the collision, atomic and electronic polarizations that for convenience are lumped together as the ε_∞ value. The complex permittivity can be separated into its real and imaginary parts as follows:

$$\varepsilon' - \mathrm{i}\varepsilon'' = \varepsilon_\infty + \frac{(\varepsilon_0 - \varepsilon_\infty)(1 - \mathrm{i}\omega\tau)}{(1 + \mathrm{i}\omega\tau)(1 - \mathrm{i}\omega\tau)} \tag{7.10}$$

$$= \varepsilon_\infty + \frac{(\varepsilon_0 - \varepsilon_\infty) - \mathrm{i}\omega\tau(\varepsilon_0 - \varepsilon_\infty)}{(1 + \omega^2\tau^2)} \tag{7.11}$$

Separating the variables gives

$$\varepsilon' = \varepsilon_\infty + \frac{(\varepsilon_0 - \varepsilon_\infty)}{(1 + \omega^2\tau^2)} \tag{7.12}$$

$$\varepsilon'' = \frac{(\varepsilon_0 - \varepsilon_\infty)\omega\tau}{(1 + \omega^2\tau^2)} \tag{7.13}$$

Equations (7.12) and (7.13) describe the ideal relaxation process in which it is assumed that all the dipoles are in similar environments and that they all relax with the same time constant. A number of semi-empirical relationships have been proposed to help with the description of the experimental curves in terms of appropriate equations. The most general is that due to Havriliak and Negami:[8]

$$\varepsilon^* = \varepsilon_\infty + \frac{(\varepsilon_0 - \varepsilon_\infty)}{\left[1 + (\mathrm{i}\omega\tau)^\beta\right]^\alpha} \tag{7.14}$$

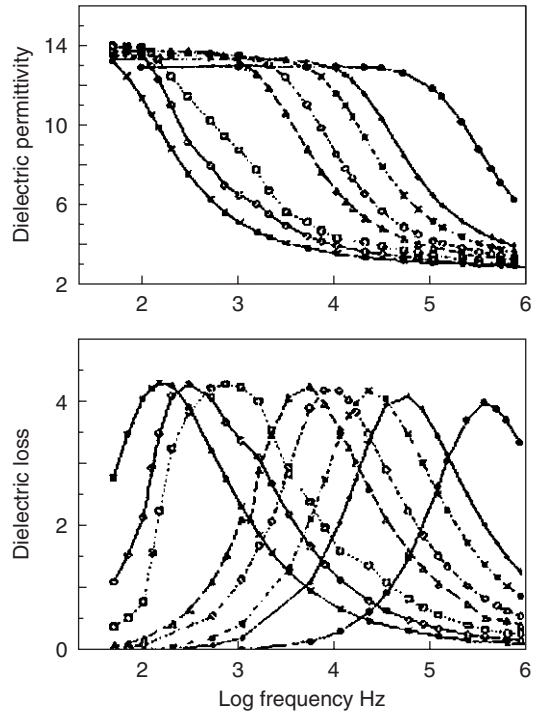

Figure 7.6 A typical set of dielectric relaxation curves of a simple dipole relaxation process.[8]

where α and β are distribution parameters. These parameters are an indication of the breadth of the distribution (β) and the possibility of there being more than one process contributing to the overall relaxation (α). A more complete discussion of the interpretation of these parameters can be found elsewhere.[8] An example of a typical dielectric relaxation is shown in Figure 7.6. As the temperature is lowered the peak in the dielectric loss moves to lower frequency reflecting the slowing down of the relaxation process. The temperature dependence of the relaxation time is determined by the kinetics of the reorientation process and is a reflection of the force field acting on the dipole.

Relaxations tend to divide into two types: those that obey a simple Arrhenius temperature dependence and those that do not. For simple thermally activated processes Arrhenius behaviour is observed. The probability of the dipole reorientating depends directly on the thermal energy distribution. The relaxation time is related to the frequency of maximum dielectric loss:

$$\tau = \frac{1}{2\pi f_{\max}} \tag{7.15}$$

and

$$f_{\max} = A_1 \exp\left(-\frac{\Delta E^{+}}{RT}\right) \tag{7.16}$$

where A_1 is the pre-exponential factor and is a function of the activation mechanism, ΔE^+ is the activation governing the reorientation process, R is the gas constant and T is the temperature. Equation (7.16) indicates that $\log(f_{max})$ plotted against $1/T$ should be linear with a slope of $-\Delta E/RT$. This type of behaviour is observed for dipoles that are able to move independently of one another, such as in a simple liquid, or for a dipole pendant to the main chain such as in the case of the methacrylate group in PMMA and is designated the β process:

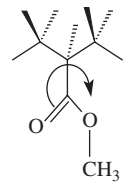

The arrow indicates that the carbonyl dipole is rotating relative to the main chain, which is fixed in space. This type of behaviour is observed at low temperature, below T_g of PMMA.

Studies of the dielectric relaxation process in the region of T_g show that the frequency–temperature dependence is not of Arrrhenius type (Figure 7.7). The process being observed corresponds to the rotation of the ester group around the polymer backbone and is designated the α process:

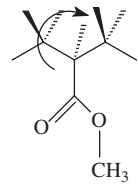

This simplistic representation of the process does not adequately describe the fact that for one ester group to move requires the co-operative motion of the

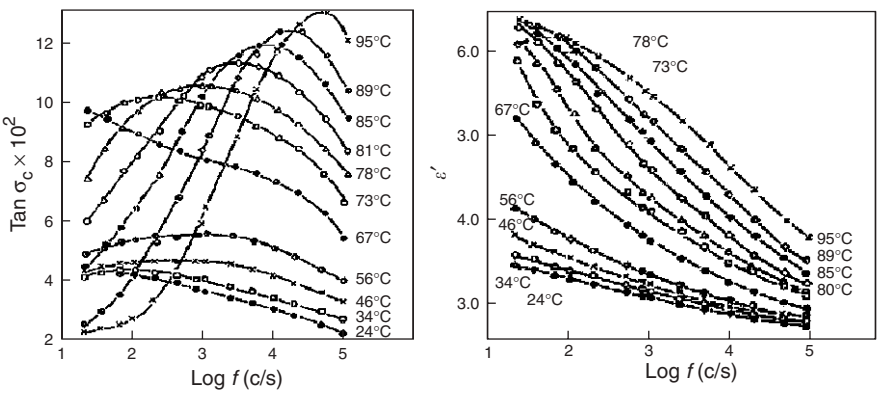

Figure 7.7 The dielectric relaxation of isotactic poly(methyl methacrylate) measured at a number of temperatures.[9]

groups around it. This co-operative process is the basis of the glass transition process and gives rise to the deviation from linearity of the temperature dependence of the relaxation process.

The dielectric relaxation for PMMA is complex at high temperatures and has been shown to be a merge of the relaxation of the side chain β process with the α process. This observation illustrates that the relaxation process reflects the motion of the dipole and this is controlled by a potential energy surface of the type discussed in Chapter 1. At higher temperatures the chain motion has more energy and the possibility of more complex, *coupled*, motions becomes possible. In the case of PMMA the side chains and backbone motions become coupled and it becomes difficult to distinguish unambiguously between the side chain and backbone motions.

7.2.3 Positron Annihilation Lifetime Spectroscopy (PALS)

Further insight into the nature of the glass transition has been obtained using the PALS technique. The natural radioactive decay of ^{22}Na produces a positron (positive electron, e^+) with energy of ~ 1.54 MeV and an accompanying γ-ray. This high-energy particle entering organic matter will be slowed down by collisions and the ionization of atoms in its path. There are three processes which can occur: (1) the positron can decay by collision; and (2) the positron can combine with an electron liberated from one of the atoms by inelastic collision and form a para spin positronium p-Ps ($Ps = e^-$ plus e^+ pair); or (3) form an ortho spin positronium (o-Ps). The p-Ps will decay naturally after a period of ~ 140 ps to two γ-rays. The o-Ps, however, is spin forbidden and has a predicted lifetime of ~ 60 ns. Both p-Ps and o-Ps can only be formed if they can achieve energies comparable to kT and find atomic vacancies within the solid or liquid in which they are formed. It is possible to analyse the decay data and abstract from the total decay a component that is associated with the o-Ps decay and ascribe this to *pick off annihilation*. The o-Ps which is spin forbidden can exchange its electron with an electron on an atom of a molecule which forms the walls of the cavity in which the o-Ps is formed. This exchange process has been explored and it has been shown that the intensity of the decay is related to the number density of the voids in the material, and the lifetime to the size.[10] A number of studies of the glass transition have been carried out, as typified by the behaviour of oligomeric phenyl ethers[8] (Figure 7.8).

Below the glass transition temperature, 230 K, the lifetime is weakly temperature dependent. Above T_g, the lifetime increases to a point T_r whereupon the rate of increase slows down. The intensity of the o-Ps component grows in an approximately linear fashion and does not perceptibly change at T_r. The observation of T_r is an intrinsic feature of T_g. As we have seen from the dielectric relaxation studies, the T_g process is associated with reorientation of dipoles about the backbone of the chain. The o-Ps will reside in a cavity formed from the surrounding polymer chains for a time that is dictated by its exchange lifetime. If, however, during this lifetime the polymer chains which form the

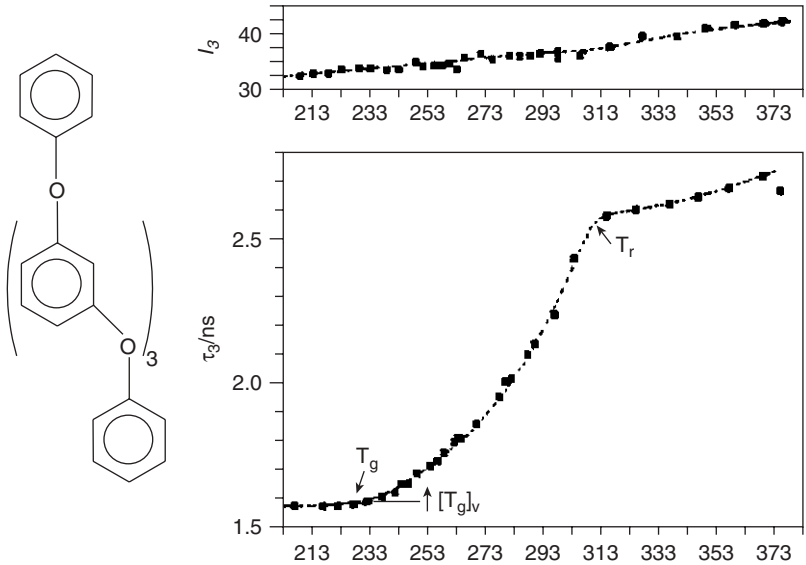

Figure 7.8 Variation of the o-Ps lifetime τ_3 and intensity I_3 as a function of temperature for an oligomeric *m*-phenoxy ether.[11,12]

walls of the cavity are able to move and effectively reduce the size of the cavity, then the effect that this will have on the o-Ps lifetime is to reduce the observed value from that which would be expected in terms of the temperature variation of the void size. This reduction in the apparent void size as a consequence of the rotational motion of the molecules is identified as T_r. A comparison of the dielectric relaxation and o-Ps lifetime behaviour (Figure 7.9) illustrates this feature of T_g.

It is apparent from comparison of the results of the above observations that the glass transition process is associated with the collective motion of elements of the polymer backbone about the polymer axis. For this motion to be able to occur there must exist in the neighbourhood of the moving segment a lack of material, voids, or as it is usually termed, *free volume*. The free volume is therefore the amount of volume required for co-operative motion about the backbone to occur.

7.3 Free Volume and the Williams–Landel–Ferry Equation[13]

The free volume theory is based on the concept introduced by Doolittle which describes the nonlinear behaviour of the viscosity of a liquid as T_g is approached:

$$\eta = A \exp\left(\frac{BV_o}{V_f}\right) \tag{7.17}$$

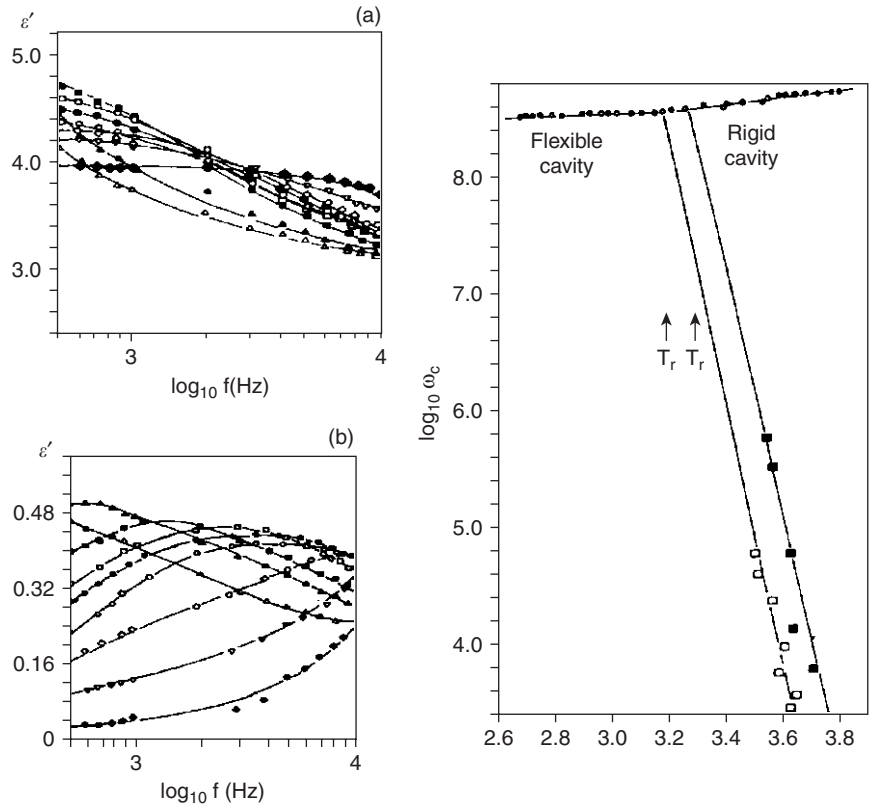

Figure 7.9 Temperature dependence of the dielectric relaxation in the oligomeric phenyl ether shown in Figure 7.8, and a comparison of the effective lifetimes indicating rigid and flexible cavity annihilation behaviour for o-Ps.[11,12]

where η is the viscosity, V_o and V_f are, respectively, the occupied and free volumes and A and B are constants for a particular system. Taking the logarithm of eqn (7.17) one obtains:

$$\ln(\eta) = \ln(A) + \frac{BV_o}{V_f} \tag{7.18}$$

We can now define a parameter f:

$$f = \frac{V_f}{(V_o - V_f)} \cong \frac{V_f}{V_o} \quad \text{since} \quad V_o \gg V_f \tag{7.19}$$

One can rewrite eqn (7.18) as

$$\ln(\eta) = \ln(A) + B\frac{1}{f} \tag{7.20}$$

The value of the parameter f can be defined as f_g at the glass transition temperature and allowed to increase with a value α_f which is equal to the liquid

expansion minus that of the glass:

$$f_t = f_g + \alpha_f (T - T_g) \tag{7.21}$$

The viscosity at any temperature T divided by the value at the glass transition temperature is then expressed by

$$\ln\left(\frac{\eta_T}{\eta_{T_g}}\right) = \ln(a_T) = B\left(\frac{1}{f_T} - \frac{1}{f_g}\right) \tag{7.22}$$

where a_T is the so-called *shift factor*. Inserting eqn (7.21) in eqn (7.22) leads to

$$\begin{aligned} \log(a_T) &= B\left(\frac{1}{f_g + \alpha_f (T - T_g)} - \frac{1}{f_g}\right) \\ &= \frac{B}{f_g}\left[\frac{f_g - f_g - \alpha_f (T - T_g)}{f_g + \alpha_f (T - T_g)}\right] \\ &= -\frac{B}{f_g}\frac{T - T_g}{(f_g/\alpha_f) + (T - T_g)} \\ &= -\frac{B'}{2.3 f_g}\frac{T - T_g}{(f_g/\alpha_f) + (T - T_g)} \end{aligned} \tag{7.23}$$

The Williams–Landel–Ferry (WLF) equation has the form

$$\log(a_T) = -17.4\frac{(T - T_g)}{51.6 + (T - T_g)} \tag{7.24}$$

The constants 17.4 and 51.6 are nearly universal and can be used to describe the behaviour of a wide range of materials. The value of 17.4 for the first constant implies that the fractional free volume at T_g is 0.025, *i.e.* of the order of 2.5% for most materials. The second constant 51.6 is the ratio f_g/α_f and this would arise if the value of α_f were equal to $4.8 \times 10^{-4}\ K^{-1}$. There are several other theories that exist, but despite its simplicity the WLF theory has been found to be very successful in describing a significant volume of data.

The WLF theory describes the shifts in the dielectric data as a function of temperature and explains the observed nonlinear dependence on temperature. The α process is therefore not controlled by thermal activation but is a function of the *free volume*. For the segment of the chain containing the dipole to move, it must have sufficient *free volume* to execute the motion.

7.4 How Big is the Element That Moves in the T_g Process?

Whilst the size of the element that moves depends on the detailed stereochemistry of a particular polymer, it is appropriate to consider how big the element might be. Direct experiment evidence can be obtained by examining the

^{13}C NMR and ultrasonic relaxation behaviour of a simple α-methylstyrene–alkane copolymer system:[13]

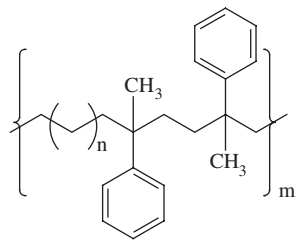

The ^{13}C NMR relaxation allows differentiation between the motion of the phenyl and methyl groups and the backbone alkane chain. By studying the temperature dependence of the relaxation times for the various groups it is possible to explore the way in which the activation energy changes with the value of n, the number of CH_2 groups joining the styrene dimers (Figure 7.10).

The relaxation with $n = 0$ approximates to the behaviour of polystyrene in solution. Once the value of n is greater than ~ 5 the motions have become decoupled and the relaxation of the alkane block is almost independent of that of the styrene dimer. This implies that the size of the group in solution that is required for co-operative motion is approximately 5–6 carbon atoms. Similar analysis has been carried out on solid-state relaxations and it is generally found that the α process involves motion of between 6 and 10 bonds depending on the polymer system. If we consider the co-operative motion of such an element it is possible to envisage that rotation about the backbone can occur without the

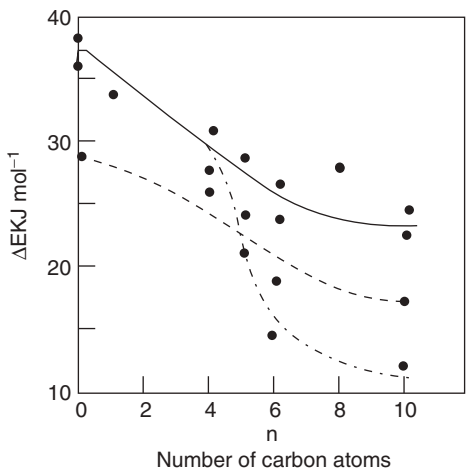

Figure 7.10 Variation of the activation energy for the various groups with the number of carbon atoms in the alkane block: – – –, methyl motion; - · - · -, styrene motion; —, alkane motion.

requirement for there to be significant translational motion of the main chain. Motion of a smaller element would require translational motion of the chain and is only possible close to chain ends:

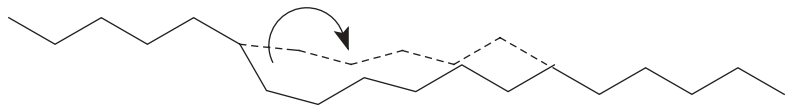

Clearly for this type of motion to occur there will have to be *free volume* next to the elements of the chain that moves. This is consistent with the concepts of the WLF theory.

7.5 Physical Characteristics of T_g

7.5.1 Factors Influencing the Value of T_g

There are a variety of different factors that will influence T_g of a material. As indicated above, it is not an individual barrier to internal rotation that determines the glass transition or the α relaxation process. The value of $\sim$80–100 kJ mol^{-1} for polystyrene is several times the value which would be predicted for rotation about an isolated bond. This observation is consistent with the rotational process involving the co-operative motion of a number of individual bonds. As indicated above, the process involves the solid expanding to create the *free volume* that is necessary for the rotational process to occur. The chains will interact through a range of forces and the overall packing density will be controlled by the *cohesive energy density (CED)* that is a measure of the chain–chain interactions. The CED[14] is equal to the vaporization energy divided by the molar volume. Polymers cannot be vaporized without degradation and the CED is determined by swelling experiments. The CED is equal to the vaporization energy of the low molecular mass liquid that swells the polymer to the greatest extent.

7.5.2 Molar Mass Effects

The molar mass of the polymer is an important factor in consideration of T_g. Since *free volume* is a rate-controlling factor, it may be anticipated that the ends of the chain will be less restricted than the central portion in terms of their ability to move. It is found empirically that the molar mass dependence for a large number of polymers can be described by the following simple relationship:

$$T_g(M) = T_g(\infty) - \frac{K}{M} \tag{7.25}$$

where $T_g(\infty)$ is the limiting high molar mass value of T_g and K is a constant which for many polymer systems has a value of $\sim 10^5$. A plot of $T_g(M)$ against

$1/M$ will be linear with a slope of $-K$. PMMA[15] has a value of 2.1×10^5 °C mol g^{-1} whereas polystyrene[16] has a value of 1.7×10^5 °C mol g^{-1}.

7.5.3 Plasticization Effect

The addition of a diluent will increase the *free volume* and consequently can lower the value of T_g. Assuming that the polymer and diluent can both be described by eqn (7.21), and using the subscripts p and d to designate, respectively, polymer and diluent, the free volume of a mixture can be expressed by

$$f_T = 0.025 + \alpha_{fp}(T - T_{gp})V_p + \alpha_{fd}(T - T_{gd})V_d \tag{7.26}$$

where V_p and V_d are, respectively, the volume fractions of polymer and diluent. At the glass transition temperature f_T becomes equal to 0.025 and T becomes equal to T_g. Rearranging eqn (7.26) gives:

$$T_g = \frac{\alpha_{fp}V_pT_{gp} + \alpha_{fd}(1 - V_p)T_{gd}}{\alpha_{fp}V_p + \alpha_{fd}(1 - V_p)} \tag{7.27}$$

In cases where the values of α_{fd} and T_{gd} are known, a very good fit to the above equation is often found. Deviations are sometimes observed and reflect specific interactions between the diluent and the polymer.

A PALS study of plasticization of PMMA with dicyclohexylphthalate illustrates the changes that occur when plasticization of a polymer occurs (Figure 7.11).

The incorporation of a low level of plasticizer fills the available *free volume*, the lifetime of the o-Ps is decreased and the temperature to which the solid has to be raised before polymer backbone motion can occur is increased. The phenomenon of the addition of a diluent raising T_g is called *antiplaticization* and is commonly observed for low levels of plasticizer. Further increase in the plasticizer levels leads to a decrease in the temperature at which the lifetime plots change slope indicative of plasticization of the polymer by the diluent.

7.5.4 Incorporation of Comonomer and Blends

In order to increase the range of physical properties available it is desirable to create polymers in which two different monomers are randomly incorporated into the polymer chain. The random copolymer will have a glass transition which is intermediate between those of the homopolymer and can be described by the simple relationship

$$\frac{1}{T_g} = \frac{W_1}{T_{g_1}} + \frac{W_2}{T_{g_2}} \tag{7.28}$$

where W_1 and W_2 are, respectively, the weight fractions of monomer (1) and (2) in the copolymer that have T_g values $_{g_1}$ and $_{g_2}$. This general mixing law is found to apply for a wide range of materials.

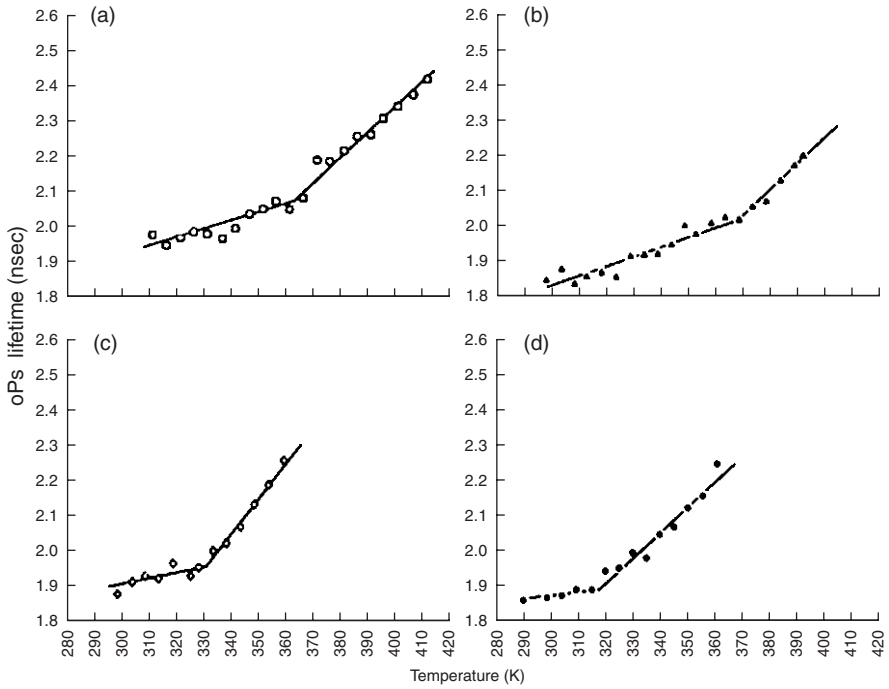

Figure 7.11 Influence of dicyclohexylphthalate on PMMA; measurement of the o-Ps lifetimes: (a) 100% PMMA, (b) 95% PMMA, (c) 90% PMMA and (d) 80% PMMA.

7.5.5 Effects of Chemical Structure

The primary barrier to internal rotational about the backbone will be determined by local interactions between neighbouring groups attached to the bonds about which rotation takes place. Values of T_g for a range of polymers are summarized in Table 7.1.

An extensive tabulation of the T_g data exists in the *Polymer Handbook*. Inspection of the literature indicates that there are a number of values quoted for the same material. The general confusion that appears to exist in relation to T_g is that it is a dynamic entity and hence is subject to the method of measurement. Hence change in the heating rate for the DSC measurement will give a different value as a consequence of the different heating rate representing a different effective frequency of observation. All the values of T_g will be interrelated through the WLF or an equivalent equation. This problem is discussed in the next section.

The mobility of the polymer chains is primarily affected by the barrier to rotation around the chain backbone. The influence of change in structure can be illustrated by considering the effect of substitution in the structure $-(CH_2-CHX)_n-$. If X = H, T_g is approximately $-60\,^{\circ}C$. Changing X to a CH_3 group increases T_g to $-10\,^{\circ}C$ and introduction of a phenyl group raises T_g further to

Table 7.1 Glass transition temperatures for a range of polymeric materials.[17,18]

Monomer	T_g *(K)*	*Monomer*	T_g *(K)*
Ethylene	195	Cyanomethyl acrylate	296
Propylene (isostatic)	272	Chloroprene (1,4 *trans*)	238
Propylene (syndiotactic)	265	Vinyl chloride (syndiotactic)	371
Propylene (atactic)	242	Vinyl acetate	307
But-1-ene (isotactic)	223	Amylose triacetate	440
Isobutylene	202	Amylose tributyrate	365
4-Methylpentane (isotactic)	373	Amylose triproprionate	406
Styrene	373	Vinyl ether ether	230
α-Methylstyrene	375	Dimethyl siloxane	150
Butadiene (1,4 *cis*)	218	Vinyl methyl ether	242
Butadiene (1,4 *trans*)	215	Acrylic acid	378
Methyl acrylate (isotactic)	311	Vinyl fluoride	313
Methyl acrylate (atactic)	378	Vinylidene fluoride	333
Methyl acrylate (syndiotactic)	378	Chlorotrifluoroethane	373
Ethyl methacrylate	338	Tetrafluoroethane	390
Butyl methacrylate	293	Ethylene terephthalate	338
Propyl methacrylate	308	Ethylene oxide	232
Hexyl methacrylate	268	Cellulose triacetate	473

100 °C. Substitution in the phenyl ring at the α-position raises T_g to 115 °C. T_g in the case of a naphthalene substitution has a value of 135 °C. T_g for biphenyl is 145 °C. T_g of the more sterically hindered poly(α-methylstyrene) is 175 °C and that of polyacenaphthalene is 265 °C. A further illustration of the influence of subtle changes on T_g can be seen in the case of poly(butyl methacrylate)s. The normal butyl methacrylate has a T_g value of −56 °C, that of secondary butyl methacrylate is −22 °C and that of isobutyl methyacrylate is 43 °C. Once more, the greater the steric interaction the higher the value of T_g.

In general terms:

- Increasing the steric hindrance for rotation about the backbone will lead to an increase in the observed value of T_g.
- Long non-polar side chains will effectively plasticize the structure and will lead to a lowing of T_g.
- Regular structures appear to have higher values of T_g than irregular structures, provided that the former do not represent a more sterically hindered situation. This situation is exemplified by a comparison of the isotactic, syndiotactic and atactic form of PMMA. The isotactic form is sterically hindered and has the lowest value of T_g. The syndiotactic and atactic forms are less sterically hindered and have higher barriers to rotation and higher values of T_g. Calculation of the rotational isomeric potentials for rotation provides a good indication of the T_g values.
- Incorporation of phenyl groups in the backbone will increase the value of T_g through conjugation effects.
- Introduction of heteroatoms, oxygen, sulfur, *etc*., will lower T_g by increasing the bond angles and reducing the steric interactions.

Poly(dimethyl siloxane) has one of the lowest values of T_g, the O–Si–O bond angle being larger and the bond lengths greater than in a carbon backbone polymer.

- The value of T_g depends on the molecular mass of the polymer, being lower for the lower molar mass materials and reaching a limiting value for molar masses typically above 10^5 Da.
- Inclusion of features in the polymer backbone that disrupt the ability for neighbouring chains to interact will in general lower T_g.

7.6 Kauzmann Paradox

Most discussions of the glass transition raise the question as to whether the process is truly a thermodynamic (second-order) transition or whether it is a kinetic phenomenon which saves the thermodynamic 'catastrophe'. There continues to be much debate about this point which illustrates the lack of the ability of a number of researchers to accept the metastable nature of the glassy state. One way of looking at a glass is to consider it having frozen-in disorder which can relax, but if T_g is sufficiently high, $\sim 200\,^{\circ}C$ or greater, we are talking about geological times scales for the process. Kauzmann examined the thermodynamic behaviour of supercooled glass-forming liquids by extrapolating their equilibrium properties to low temperature. He found that not very far below the glass-forming temperature but still above 0 K the extrapolated entropy and several other properties of the liquid become less than that of the crystalline solid and highlight the fact that the liquid properties become less than the crystal state properties above 0 K.

7.6.1 Pressure Dependence of the Glass Transition

Typical PVT data for a glass-forming polymer are shown in Figure 7.12. It is apparent that as the pressure is increased so the specific volume is reduced and there is a corresponding increase in the value of T_g. This type of behaviour is generally found for most polymers. As we will see later, the exact behaviour is dictated by the cooling regime that is adopted.

7.6.2 Physical Ageing

Recognizing that T_g has a kinetic component because it is associated with co-operative motion of the elements of the lattice structure moving to create *free volume* for the molecules or polymer chains to move, leads to the idea that T_g can change with storage time. Figure 7.13 indicates the isothermal contraction of glucose after quenching from $T_0 = 40\,^{\circ}C$ to different temperatures.

Glucose, like all glass-forming liquids, exhibits *physical ageing*. Depending on the extent to which cooling takes place, the rate of the physical ageing will vary. The common feature of all glasses is that this behaviour is nonlinear and does not follow a simple Arrhenius type of behaviour. The process involves

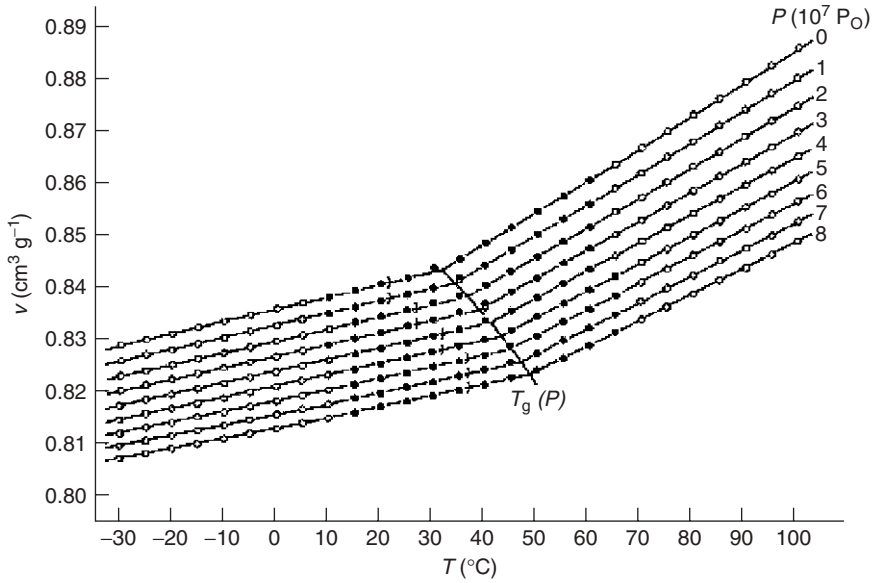

Figure 7.12 The specific volume of poly(vinyl acetate) measured as a function of temperature for pressures between 1×10^7 and 8×10^7 Pa (from reference 19).

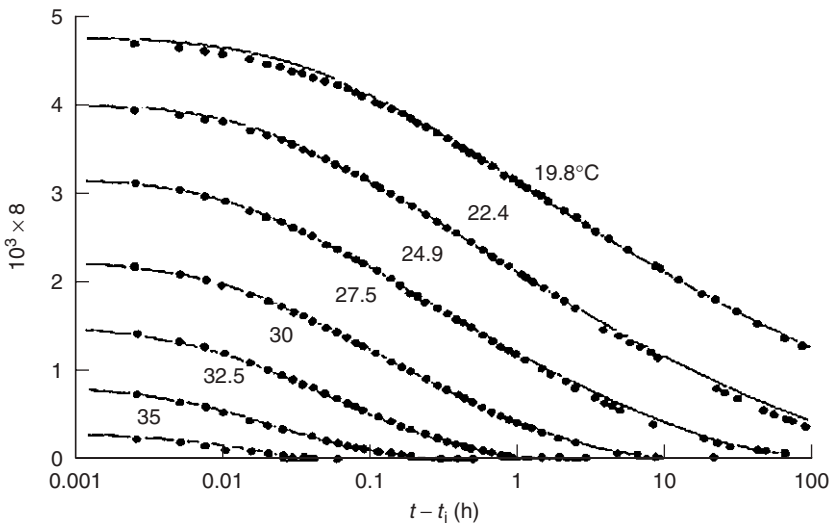

Figure 7.13 Quenching behaviour of glucose cooled from 40 °C.[5]

rearrangement of the organization of the species in the glass and as such will involve a redistribution of *free volume* in the system and hence one would expect it to be controlled by a WLF or similar type of relationship. Similar behaviour can be observed in respect to creep. If a sample is subjected to a load,

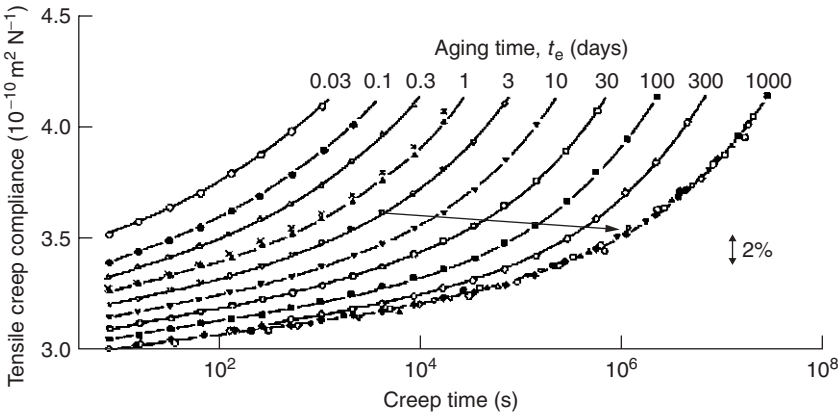

Figure 7.14 Creep behaviour for poly(vinyl chloride).[5]

then after a period of time the sample will deform. The behaviour for poly(vinyl chloride) is shown in Figure 7.14.

All the physical ageing phenomena can be understood as the slow relaxation of the configurational entropy that is frozen into the glass on quenching below T_g. In the case of the simple system *ortho*-terphenyl, the ageing process goes to completion and crystals are formed. With most polymeric materials the development of order is limited and densification is the best description of the process. An extensive review of this topic is to be found in Struick's book.[5]

7.7 Distribution of Free Volume in a Glass

In order to understand many of the properties of the glassy state it is important to consider the nature of *free volume*. The WLF theory is based in the concept of free volume V_f (eqn (7.19)) and leads to a universally accepted and successful method of describing the behaviour of glasses. The question must be asked as to whether *free volume* is a single-valued function at a particular temperature and pressure or whether it is a distribution of values and the WLF parameter is strictly speaking an averaged parameter. Some insight into this problem can be obtained by studying the rate of ring closure of indolinobenzospirans when dispersed in a polymer matrix:

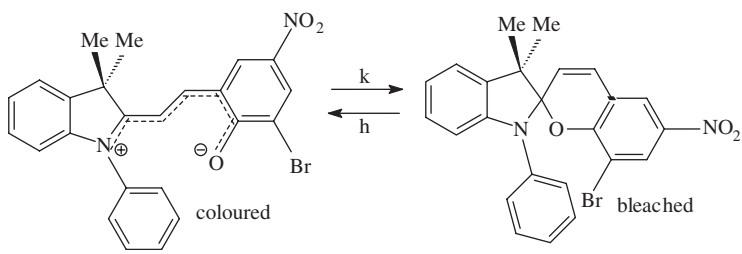

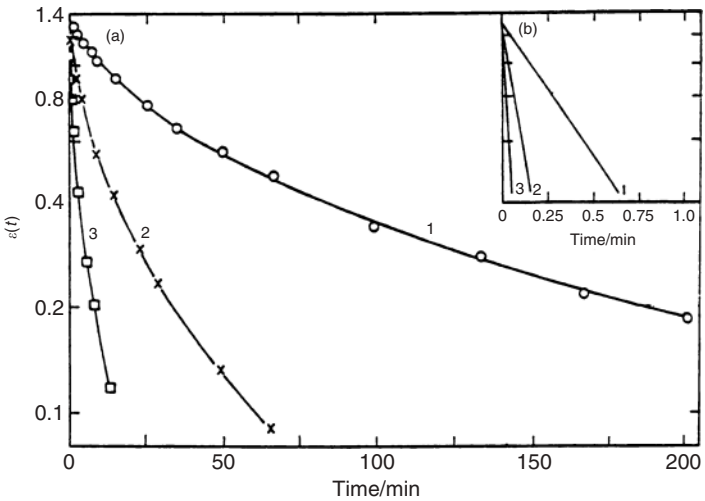

Figure 7.15 Kinetic plots for the ring closure reaction for 8-bromo-2,2′-dimethyl-6-nitro-1′-phenyl-(2H-[1]benzospiropyran-2,2′-indoline) in PMMA at (1) 17 °C, (2) 30.2 °C and (3) 42.0 °C.

Exposure of the 8-bromo-2,2′-dimethyl-6-nitro-1′-phenyl-(2H-[1]benzospiropyran-2,2′-indoline) to light causes it to isomerize into the coloured form. In a solvent it rapidly converts to the bleached form and exhibits first-order kinetics.[20] The process is thermally activated and will require volume for the relative rotation of the two parts of the molecule to effect ring closure. However, if the same process is carried out with the dye in a polymer matrix the process now depends on there being *free volume* available for the rotation of the molecule required for ring closure to occur. Studies of the kinetics (Figure 7.15) indicate that simple kinetics is no longer followed and that a more complex analysis is required. Good fits of the data can be obtained if it is assumed that the process is split into two processes. The initial fast decay is essentially the same as that seen in a liquid and indicates that the ring closure process is only subject to thermal control. This implies that these molecules have sufficient *free volume* available to execute the process.

The longer time kinetics has to allow for the *free volume* being created next to the molecule to allow for the ring closure. To describe the process it is necessary to allow for there to be a distribution of *free volume* in the system and this is best described by a distribution function $Z(p)$ which has the form

$$Z(p) = \exp(\beta\sqrt{B}) \exp(-Bp)\psi(\beta, p) \tag{7.29}$$

where B describes the kinetics of the ring closure process and p is the probability of the occurrence of the chromophore in a matrix region of sufficient free volume for ring closure to occur. Analysis of a number of chromophores indicates that this type of function allows for the *free volume*

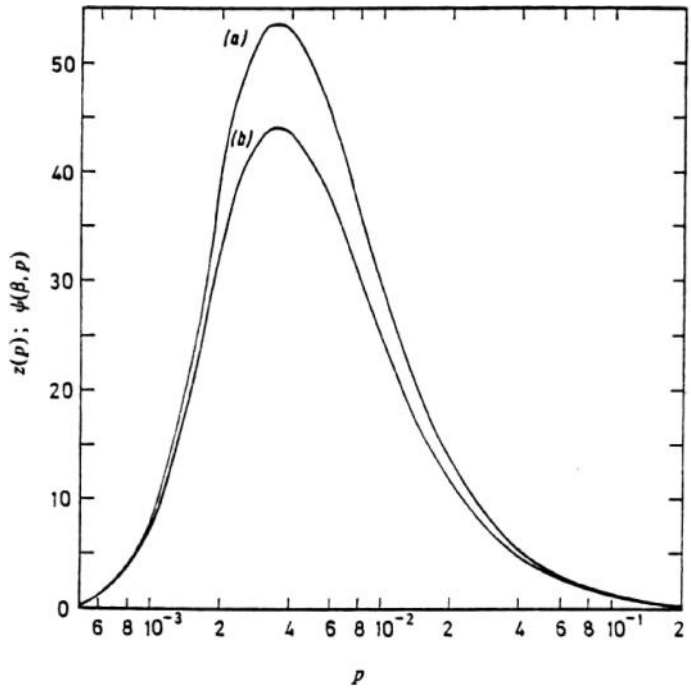

Figure 7.16 Functions (a) $Z(p)$ and (b) $\psi(\beta, p)$ using $B = 2$, $\beta = 0.146$, the values of these parameters having been derived from kinetic data obtained at 17 °C for the system discussed in the text.

distribution and has the form shown in Figure 7.16. The parameter β is the distribution parameter. This experiment illustrates that rather than being single valued, *free volume* is more correctly described by a distribution of values. In a matrix there will be voids which are smaller and larger than a mean value, the latter being the value which is usually described by the WLF equation. If we accept that *free volume* is a distribution then this has profound implications for the way we look at other features of the glassy phase in materials.

If *free volume* is a distribution rather than being single valued then the dynamic, time-dependent, behaviour would conform to a single relaxation process and have an ideal form. However, if there is a distribution of sites at which relaxation can occur with different values of the *free volume*, then there will be a distribution of relaxation times. This is what is observed experimentally and produces the form of the curves shown in Figure 7.13 and 7.14.

7.8 Fragility

It has been observed that for all glasses it is possible to define a *relaxation time* associated with the reorganization of the liquid–glass structure. The relaxation

time, which has a theoretical value of infinity at T_K, a temperature just below T_g, decreases with increasing temperature to the value of 200 s at the 'normal' accepted glass transition temperature,[21] and then continues to fall as $T > T_g$ in a manner which is usually predicted from the Vogel–Fulcher–Tammann (VFT) equation:

$$\tau = \tau_0 \exp\left(\frac{DT_0}{T - T_0}\right) \tag{7.30}$$

where τ_0, D and T_0 are constants; $T_0 \sim T_K$ ($< T_g$) is the divergence temperature. A plot of the reduced temperature dependence of relaxation times for several weak and strong forming glasses is shown in Figure 7.17. Deviations from Arrhenius behaviour indicated by the dotted line are an indication of the strength of the interactions present in the liquid. In liquids like SiO_2, BeF_2 and P_2O_5 deviations are barely detectable and these are classed as 'strong' liquids. In other systems, deviations are observed, and the apparent slope of the temperature dependence is many times the vaporization energy or in the case of polymers the bond dissociation energy; these are fragile liquids. Thermodynamically strong liquids like SiO_2 and GeO_2 show small differences in heat

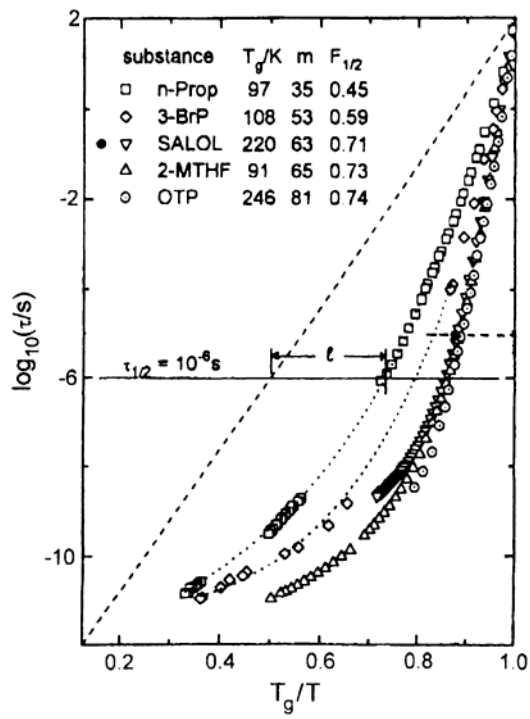

Figure 7.17 T_g scaled Arrhenius plot of the dielectric relaxation times for several glass-forming molecular liquids. The fragility $F_{1/2}$ is defined as $2(T_g/T_{1/2})$. The liquids are from top to bottom *n*-propanol, 3-bromopentane, salol (phenylsalicylate), 2-methyltetrahydrofuran and *ortho*-terphenyl.

capacity, ΔC_p, between liquid and glass and the entropies approach the crystal values only slowly. Fragile liquids have such high heat capacities relative to their crystals so that a natural extrapolation of the liquid entropy below the melting point indicates disappearance of the excess over the crystal at a temperature far below 0 K, the Kauzmann entropy catastrophe discussed above. Most polymer systems show behaviour that resembles *ortho*-terphenyl and are strong glasses.

The proximity of the divergence temperature T_0 to the 'normal' T_g ($0 < T_0/T_g < 1.0$) provides one measure of the fragility.[22] Using either the VFT or the WLF equations creates problems because these do not accommodate the 'fragility' of the material in their derivations.

A parameter m can be defined as follows:

$$m = (T_g)^{-1} \frac{\partial(\ln \tau)}{\partial(1/T)} \tag{7.31}$$

where m is the '*fragility*' or *steepness index*. Angell and co-workers[22] have proposed that the fragility can be defined in terms of a length parameter l determined as the deviation from Arrhenius behaviour at an effective relaxation time of 10^{-6} s. There is no fundamental reason for this choice; however, in the case of polymers it does correspond to a length scale which is comparable with collective motions executed by the polymer chain. As indicated above, different techniques give apparently different values for T_g. Part of the reason for this apparent discrepancy is the fact that different methods are looking at different length scales of motion of the system. A dynamic mechanical observation will obviously be expected to see a different collection of motions from those observed by dielectric or nuclear magnetic resonance studies. A more detailed discussion of this topic is presented elsewhere.[6] The origins and definitions of fragility have been extensively discussed in the literature. The main property which emerges is that fragility is an indication of the extent to which the motions are associated with T_g and co-operative in nature.

7.9 Theories of T_g

A considerable amount of research has been reported into the modelling of the glassy state and in particular attempts to predict the distribution of the relaxation processes which take place close to or just above T_g. The comparison between dynamic and thermodynamic approaches has been discussed by Wales and Doye.[23] They have used a model which is similar to that used to model crystallization. Each of the possible configurations of the species involved in glass formation are depicted in terms of a series of interconnected energy states; movement from one potential energy surface (PES) to another state is controlled by an energy barrier. It is assumed that the entities in the liquid attempting to organize themselves into a crystalline state are able to execute two types of motion: vibrations about a local minimum and less frequent jumps

over a significant barrier to form a new more stable state. Using this approach it is possible to set up a series of partition functions which allow calculation of thermodynamic properties of the system. The advantage of this approach is that it naturally predicts a distribution of relaxation times and by adjusting the energy values can accommodate both strong and weak fluids. The principal problem is that no theory helps with the visualization of the glass state, which is best assumed to be a disordered array of interacting species which interact to varying degrees and inhibit the creation of the order that would lead to crystal growth. An extensive review of the various approaches to the modelling of the relaxation behaviour of glasses has been published previously[24] and a detailed discussion of this topic is beyond the scope of the present text.

Recommended Reading

R.T. Bailey, A.M. North and R.A. Pethrick, *Molecular Motion in High Polymers*, Oxford University Press, 1982.
G.B.N. McKenna, in *Comprehensive Polymer Science*, ed. G. Allan and J. C. Bevington, Pergamon Press, 1989, p. 311.
L.C.E. Stuick, *Physical Ageing in Amorphous Polymers and Other Materials*, Elsevier, Amsterdam, 1978.

References

1. B. Wandelt, D.J.S. Birch, R.E. Imhof and R.A. Pethrick, *Polymer*, 1992, **33**, 3558.
2. R.A. Pethrick and B.D. Malholtra, *J. Chem. Soc., Faraday Trans. 2*, 1982, **78**, 95.
3. D. Campbell, R.A. Pethrick and J.R. White, *Polymer Characterization*, Stanley Thornes, Cheltenham, UK, 2000.
4. A. Eisenberg, *Physical Properties of Polymers*, American Chemical Society, Washington, DC, 1984, p. 55.
5. L.C.E. Stuick, *Physical Ageing in Amorphous Polymers and Other Materials*, Elsevier, Amsterdam, 1978.
6. R.T. Bailey, A.M. North and R.A. Pethrick, *Molecular Motion in High Polymers*, Oxford University Press, 1982.
7. R.A. Pethrick and D. Hayward, *Prog. Polym. Sci.*, 2002, **27**, 1983.
8. S. Havriliak and S.J. Negami, *Dielectric and Mechanical Relaxation in Materials*, Hanser, Munich, 1997.
9. G.P. Mikhailov and T.I. Borisova, *Polym. Sci. USSR*, 1961, **2**, 387.
10. R.A. Pethrick, *Prog. Polym. Sci.*, 1997, **22**, 1–47.
11. R.A. Pethrick, F.M. Jacobsen, O.A. Mogensen and M. Eldrup, *J. Chem. Soc., Faraday Trans. 2*, 1980, **76**, 225.
12. R.A. Pethrick and B.D. Malholtra, *Phys. Rev. B*, 1983, **22**, 1256.

13. A.V. Cunliffe and R.A. Pethrick, *Polymer*, 1980, **21**, 1025.
14. R.A. Hayes, *J. Appl. Polym. Sci.*, 1961, **5**, 318.
15. R.B. Beevers and E.F.T. White, *Trans. Faraday Soc.*, 1960, **56**, 744.
16. F. Buche, *Physical Properties of Polymers*, Wiley Interscience, New York, 1962.
17. R.J. Andrews and E.A. Grulke, in *Polymer Handbook*, ed. J. Brandrup, E.H. Immergut and E.A. Grulke, Wiley Intercsience, New York, 1999.
18. W. Kauzmann, *Chem Rev.*, 1948, **43**, 219.
19. J.E. MacKinney and M. Goldstein, *J. Res. Natl Bur. Stand. Sect. A*, 1978, **78A**, 331.
20. M. Kryzewski, B. Nadolski, A.M. North and R.A. Pethrick, *J. Chem. Soc., Faraday Trans. 2*, 1980, **76**, 351.
21. C.T. Moyniham, P.B. Macedo, C.J. Montrose, P.K. Gupta, M.A. DeBolt, J.F. Dill, P.W. Drake, A.J. Easteal, P.B. Elterman, R.P. Moeller, H.A. Sasabe and J.A. Wilder, *Ann. N. Y. Acad. Sci.*, 1976, **279**, 15.
22. J.L. Green, K. Ito, K. Xu and C.A. Angell, *J. Phys. Chem. B*, 1999, **103**, 3991.
23. D.J. Wales and J.P.K. Doye, *Phys. Rev. B.*, 2001, **63**, 214204.
24. G.B.N. McKenna in *Comprehensive Polymer Science*, ed. G. Allan and J.C. Bevington, Pergamon Press, 1999.

CHAPTER 8

Polymer Blends and Phase Separation

8.1 Introduction

In the preceding chapters, the systems considered have been essentially single components and the physical properties exhibited by these systems are determined by the chemical structure and molar mass of the molecules. Early in the commercial use of polymers, it was recognized that it was possible by mixing various monomers in the reaction to obtain polymers with different properties from those of the homopolymers. Some of these copolymers had properties that were simple averages of the properties of the homopolymers, others had different characteristics.[1,2] Rather than having to make different copolymers the possibility of generation of blends of the homopolymers was investigated. With certain pairs of polymers, homogeneous mixtures were created that had properties that were an average of those to the homopolymers; others did not form blends. As a result there has been considerable effort devoted to the study of the blending processes and the types of morphology that are created from mixing either monomers or polymers. There are a variety of different ways of describing blends. The term *compatible* is often used to describe mechanically processable blends that resist gross phase separation and/or give desirable properties. Blends that are homogeneous at some temperature may under other conditions phase separate and these are referred to as partially or nearly miscible blends. According to the above definition polymer blends can be divided into three basic groups:[3]

Group 1. Miscible blends:
- polystyrene–poly(2,6-dimethyl 1,4-phenylene oxide)
- poly(methyl methacrylate)–poly(vinylidene fluoride)

Group 2. Partially miscible blends:
- polystyrene–poly(vinyl methyl ether)
- poly(ethylene oxide)–poly(ether sulfone)
- phenoxy resin–poly(ether sulfone)

Group 3. Immiscible blends:
- polyethylene–poly(methyl methacrylate)
- polystyrene–poly(methyl methacrylate).

Some systems are made compatible by the addition of a third component that is termed a *compatibilizer* or *emulsifier*. A considerable number of studies have been carried out and it is desirable to be able to rationalize the behaviour of these systems in terms of a theoretical framework.[4]

8.2 Thermodynamics of Phase Separation

Various attempts have been made to rationalize the behaviour of multicomponent systems.[1,2] Using the classical framework of Gibbs, it is possible to understand the behaviour of many polymer blends simply by considering the change in the free energy with composition. If

$$\left(\frac{\partial^2 G}{\partial V^2}\right)_T = -\left(\frac{\partial P}{\partial V}\right)_T = 0 \tag{8.1}$$

where G is the free energy, V is the volume, P is the pressure and T is the temperature, then this defines the spinodal condition and represents a boundary between a stable single phase and one in which two phases are stable. In a homogeneous binary mixture, we can use the usual thermodynamic conventions of additivity to create the properties of the mixtures. If the system is miscible then the free energy change G with composition can be depicted by the curves shown in Figure 8.1a.

Lowing the temperature above some critical value T_c may lead to a variation as depicted in Figure 8.1b. Since the laws of dilute solutions require $G_m(x_2)$ to have an infinite slope at both ends of the x_2 axis, and negative at $x_2 = 0$ and positive at $x_2 = 1$, there must be two positively curved portions of the $G_m(x_2)$ curve surrounding a negatively curved portion, separated by two points of inflection at the compositions x_{2s1} and x_{2s2}. Between these two compositions a

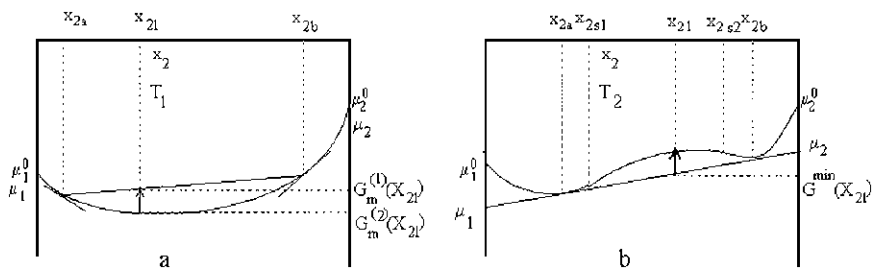

Figure 8.1 Isobaric $G_m(x_2)$ curves for a partially miscible binary mixture: (a) above the critical temperature; (b) below the critical temperature.

single-phase system will separate spontaneously because any concentration fluctuation, however small, will reduce G_m and so trigger further separation until the minimum value is reached at G_m^{min} (x_{21}). Such a separation is called a spinodal decomposition, the two points of inflection being known as spinodal points and defined by

$$\left(\frac{\partial^2 G_m}{\partial x_2^2}\right)_{P,T} = 0 \quad \text{(spinodal)} \tag{8.2}$$

and the condition for *instability* is

$$\left(\frac{\partial^2 G_m}{\partial x_2^2}\right)_{P,T} < 0 \quad \text{(unstable)} \tag{8.3}$$

The ranges (0, x_{2a}) and (x_{2b}, 1) are stable regions and the remaining ranges (x_{2a}, x_{2s1}) and (x_{2s2}, x_{2b}) are called metastable because, although as homogenous systems they have a larger G_m value than the two phases value represented by the line $\mu_1\mu_2$, they are still stable with respect to immediately neighbouring concentrations in the sense of Figure 8.1a. Metastable systems require some form of nucleation to reach their stable two-phase state. Unstable systems can do so without nucleation.

8.2.1 Thermodynamics of Polymer–Polymer Miscibility

The theoretical modelling of the behaviour of simple liquids and polymers can be approached from consideration of the systems as behaving like gases and as solids. The first group of theories are commonly referred to as *equation of state* theories and assume that the gas laws can be adapted to describe the behaviour of liquids. Flory and co-workers proposed an equation of state theory for the thermodynamics of polymer melts in which they blended the two approaches.[1] Each of the pure components is characterized by three state parameters, V^*, T^* and P^*, that can then be used using conventional thermodynamic expression to obtain density, thermal expansion coefficients and thermal pressure coefficients. In polymer mixtures, two additional terms were introduced, X_{12} and Q_{12}, associated with the enthalpy and entropy of the mixture and describe specific interactions between the two components. Mixing two components can give rise to additional interactions not present in either of the components. For instance, poly(vinyl alcohol) will undergo hydrogen bonding interactions with poly(methyl acrylate) and an additional term is required to account for the additional interactions. It is normal to describe a set of reduced thermodynamic variables:

$$\tilde{V} = V/V^*; \quad \tilde{T} = T/T^* = kT/z\varepsilon; \quad \tilde{P} = P/P^* = PV^*/z\varepsilon \tag{8.4}$$

which are respectively the volume, temperature and pressure, z is the coordination number of the equivalent lattice and k is the Boltzmann constant. The

subscripts 1 and 2 are used in the following derivation to designate the two components of the mixture. The resulting equation of state is

$$\frac{\tilde{P}\tilde{V}}{\tilde{T}} = \frac{\tilde{V}^{1/3}}{(\tilde{V}^{1/3} - 1)} - \frac{1}{\tilde{T}\tilde{V}} \tag{8.5}$$

At atmospheric pressure where $\tilde{P} \sim 0$ this equation becomes

$$\tilde{T} = \frac{(\tilde{V}^{1/3} - 1)}{\tilde{V}^{4/3}} \tag{8.6}$$

The $\tilde{V}$ of the mixture can be related to the thermal expansion α by

$$\alpha = \left(\frac{1}{V}\right)\left(\frac{\partial V}{\partial T}\right) \tag{8.7}$$

or

$$\alpha T = \left(\frac{\tilde{T}}{\tilde{V}}\right)\left(\frac{\partial \tilde{V}}{\partial \tilde{T}}\right)_P \tag{8.8}$$

The two terms in this equation are obtained from eqn (8.6) to give

$$\alpha T = \frac{3(\tilde{V}^{1/3} - 1)}{(4 - 3\tilde{V}^{1/3})} \tag{8.9}$$

or

$$\tilde{V}^{1/3} = \frac{(3 + 4\alpha T)}{(3 + 3\alpha T)} \tag{8.10}$$

The thermal pressure coefficient γ can be obtained as follows:

$$\gamma = \left(\frac{\partial P}{\partial T}\right)_V = \frac{P^*}{T^*}\left(\frac{\partial \tilde{P}}{\partial \tilde{T}}\right)_{\tilde{V}} \tag{8.11}$$

The parameter $(\partial \tilde{P}/\partial \tilde{T})_{\tilde{V}}$ is evaluated by differentiating eqn (8.5) with respect to $\tilde{T}$ at constant $\tilde{V}$. Substitution in eqn (8.11) and combining with eqn (8.6) gives

$$P^* = \gamma T \tilde{V}^2 \tag{8.12}$$

The volume fractions of the constituent polymers in the mixture are given by

$$\phi_2 = \frac{m_2 V^*_{\text{sp2}}}{(m_2 V^*_{\text{sp2}} + m_1 V^*_{\text{sp1}})} \tag{8.13}$$

and

$$\phi_1 = 1 - \phi_2 \tag{8.14}$$

where m_i is the mass of component i and V^*_{spi} is its hard core volume per gram. In addition the volume fractions, site fractions, are defined as

$$\theta_2 = \left(\frac{S_2}{S_1}\right) \frac{\phi_2}{[\phi_1 + (S_2/S_1)\phi_2]} \tag{8.15}$$

and

$$\theta_1 = 1 - \theta_2 \tag{8.16}$$

where S_i is the surface area per unit volume ratio for component i which is usually calculated using Bondi's tabulations of group surface areas[4] and volumes.[2] P^* of the mixture is related to the contact interaction term X_{12} via

$$P^* = \phi_1 P^*_1 + \phi_2 P^*_2 - \phi_1 \phi_2 X_{12} \tag{8.17}$$

The X_{12} term has energy per unit volume dimensions and is concentration independent, unlike the classic Flory–Huggins interaction parameter that is dimensionless and concentration dependent. Both parameters are still temperature and pressure dependent. T^* is related to P^* through

$$\frac{P^*}{T^*} = \frac{\phi_1 P^*_1}{T^*_1} + \frac{\phi_2 P^*_2}{T^*_2} \tag{8.18}$$

These equations indicate the way in which the thermodynamic properties of the system change with the composition. In a blend of polymers, new interactions can be created which are not present in the homopolymer system. For instance, polar groups can induce dipoles or quadrupoles that will increase the interaction energy between the polymer chains and can change the entropy of the system. Such interactions explain the unusual properties obtained when fluorine atoms are present in a polymer system.

8.2.2 Enthalpy and Entropy Changes on Mixing

The enthalpy change on mixing, ΔH_M, is the difference in energy between the mixture E_{012} and the pure components E_{01} and E_{02} and is given by

$$\Delta H_M = E_{012} - (E_{01} + E_{02}) \tag{8.19}$$

Equation (8.19) can be rewritten using the above equations in the form[3]

$$\Delta H_M = (m_1 V^*_{sp1} + m_2 V^*_{sp2}) \left(\frac{\phi_1 P^*_1}{\tilde{V}_1} + \frac{\phi_2 P^*_2}{\tilde{V}_2} - \frac{P^*}{\tilde{V}}\right) \tag{8.20}$$

The enthalpy interaction parameter χ_H is obtained from the partial molar heat of mixing. For component 1 this has the form

$$\Delta\tilde{H}_1 = \tilde{H}_1 - \tilde{H}_0 = \left(\frac{\partial \Delta H_M}{\partial N_1}\right)_{T,P,N_2} = \left(\frac{\partial \Delta H_M}{\partial N_1}\right)_{N_2,T,V} + \left(\frac{\partial \Delta H_M}{\partial \tilde{V}}\right)_{N_2T_1N_1}\left(\frac{\partial \tilde{V}}{\partial N_1}\right)_{N_2,T,P} \tag{8.21}$$

and is obtained using the usual thermodynamic arguments for the expansion of standard functions. Substitution of the above equations yields

$$\begin{aligned}\Delta\tilde{H}_1 =& P_1^* V_1^*(\tilde{V}_1^{-1} - \tilde{V}^{-1}) + \left(\frac{\alpha T}{\tilde{V}}\right)\left(\frac{\tilde{T}_1 - \tilde{T}}{\tilde{T}}\right) + \frac{(V_1^* X_{12})}{\tilde{V}}(1+\alpha T)\theta_2^2 \\ =& RT\chi_H\phi_2^2\end{aligned} \tag{8.22}$$

Similarly the entropic interaction parameter, χ_S, is obtained from the partial molar excess entropy changes on mixing and is given by

$$\begin{aligned}T\Delta\tilde{S}(\text{excess}) =& -P_1^* V_1^*\left(\frac{3\tilde{T}_1 \ln(\tilde{V}_1^{1/3} - 1)}{(\tilde{V}^{1/3} - 1)} - \frac{\alpha T(\tilde{T}_1 - \tilde{T})}{\tilde{T}\tilde{V}}\right) \\ &+ \frac{V_1^*\theta_2^2(\alpha T X_{12} + T\tilde{V}Q_{12})}{\tilde{V}} = RT\chi_S\theta_2^2\end{aligned} \tag{8.23}$$

Combining eqn (8.22) and (8.23) gives the excess chemical potential of component 1 in the mixture:

$$\begin{aligned}\Delta G_1(\text{excess}) =& \Delta H_1 - T\Delta S_1(\text{excess}) = \Delta\mu_1(\text{excess}) \\ =& P_1^* V_1^*\left(\frac{3\tilde{T}_1 \ln(\tilde{V}^{1/3} - 1)}{(\tilde{V}^{1/3} - 1)} + (\tilde{V}_1^{-1} - \tilde{V}^{-1})\right) + V_1^*\theta_2^2\frac{(X_{12} - T\tilde{V}Q_{12})}{\tilde{V}} \\ =& RT\chi_e\theta_2^2\end{aligned} \tag{8.24}$$

Therefore we can deduce that

$$\chi_e = \chi_H + \chi_S \tag{8.25}$$

For a polymer system such as ethylene–vinyl acetate with 45% acetate mixed with chlorinated polyethylene with a 52% chlorine[1] content, the value of X_{12} would be -4.9 J cm^{-3} and Q_{12} has a value of -0.0108 J cm^{-3} °C^{-1}. Since χ_H is negative and χ_S is positive then χ_e is small and negative, which indicates that the mixture will be homogeneous. Experimentally it is observed that this mixture at 83.5 °C is homogeneous and becomes heterogeneous at 90 °C.[3]

8.3 Phase Separation Phenomena

Mixing two polymer systems will create a range of new interactions. In general, specific interactions are exothermic, causing negative changes in heat of mixing which in turn favours miscibility but involves a penalty in entropy. The entropy change on mixing consists of combinatorial and residual parts. The latter arise because of the specific interactions whereas the former are due to statistical mixing of the two polymers involved. The change in free energy of the system is therefore expressed as

$$\Delta G_{\mathrm{M}} = \Delta H_{\mathrm{M}} - T(\Delta S_{\mathrm{C}} + \Delta S_{\mathrm{R}}) \tag{8.26}$$

A negative free energy change is necessary but not a sufficient condition for homogeneity between two polymers. More appropriately the shape of ΔG as a function of concentration of one of its constituents at a temperature T describes homogeneity or heterogeneity of the mixture as discussed in Section 8.2.

8.3.1 The Phase Diagram for Nearly Miscible Blends

Studies of polymer solutions and binary mixtures indicate that there exist two critical temperatures: the upper critical solution temperature (UCST) and the lower critical solution temperature (LCST). The LCST is the lowest temperature for which two phases can be observed and the USCT is the highest temperature at which two phases can be observed for a mixture. The bimodal condition is described by

$$\Delta\mu_i = \Delta\mu_i(\text{combinational}) + \Delta\mu_i(\text{excess}) \tag{8.27}$$

or

$$\begin{aligned}\Delta\mu_i =& RT\left[\ln\phi_1 + \left(1 - \frac{r_1}{r_2}\right)\phi_2\right] \\ &+ P_1^* V_1^* \left[\frac{3\tilde{T}_1 \ln\left(\tilde{V}_1^{1/3} - 1\right)}{\left(\tilde{V}^{1/3} - 1\right)}\left(\tilde{V}_1^{-1} - \tilde{V}^{-1}\right) + P_1\left(\tilde{V} - \tilde{V}_1\right)\right] \\ &+ \frac{V_1^* \theta_2^2 \left(X_{12} - T\tilde{V}Q_{12}\right)}{\tilde{V}}\end{aligned} \tag{8.28}$$

and r_1 and r_2 are the lattice sites occupied by the components 1 and 2. Similarly the chemical potential of component 2 is

$$\begin{aligned}\Delta\mu_2 =& RT\left[\ln\phi_2 + \left(1-\frac{r_1}{r_2}\right)\phi_1\right] \\ &+ P_2^* V_2^* \left[\frac{3\tilde{T}_2 \ln\left(\tilde{V}_2^{1/3}-1\right)}{\left(\tilde{V}^{1/3}-1\right)}\left(\tilde{V}_2^{-1}-\tilde{V}^{-1}\right)\tilde{P}_2\left(\tilde{V}-\tilde{V}_2\right)\right] \\ &+ \frac{V_2^*\theta_1^2\left(X_{12}-T\tilde{V}Q_{12}\right)S_2}{S_1\tilde{V}}\end{aligned} \tag{8.29}$$

The spinodal is obtained by applying the stability condition. Note that two terms have been added to the equations that introduce the pressure dependence of the functions:

$$\frac{\partial^2 \Delta G_M}{\partial\phi_2} = \frac{\partial\Delta\mu_i}{\partial\phi_2} = 0 \tag{8.30}$$

Differentiating eqn (8.28) with respect to ϕ_2 gives the spinodal condition:

$$\begin{aligned}&-\frac{1}{\phi_1} + \left(1-\frac{r_1}{r_2}\right) - \frac{P_1^* V_1^*}{RT_1^*}\frac{A}{\left(\tilde{V}-\tilde{V}^{2/3}\right)} + \frac{P_1^* V_1^*}{RT}\left(\frac{1}{\tilde{V}^2}+P_1\right)A \\ &+ \frac{V_1^* X_{12}}{RT}\frac{2\theta_2}{\tilde{V}}\frac{\theta_1\theta_2}{\phi_1\phi_2} - \frac{V_1^* X_{12}}{RT}\frac{\theta_2^2}{\tilde{V}^2}A \\ &- \frac{V_1^* Q_{12}}{R}\left(\frac{2\theta_2}{\tilde{V}}\frac{\theta_1\theta_2}{\phi_1\phi_2}\right) = 0\end{aligned} \tag{8.31}$$

where

$$A = \frac{\partial\tilde{V}}{\partial\phi_2} = -\frac{\partial\tilde{V}}{\partial\phi_1} \text{ or } \frac{\partial\tilde{V}}{\partial\phi_2} = \frac{B - C\left(\frac{\tilde{P}}{\tilde{T}}+\frac{1}{\tilde{T}\tilde{V}^2}\right)}{\frac{2}{\tilde{V}^3} - \frac{\tilde{T}}{3\tilde{V}^{5/3}}\frac{\left(3\tilde{V}^{1/3}-2\right)}{\left(\tilde{V}^{1/3}-1\right)^2}} \tag{8.32}$$

and

$$B = \frac{\partial\tilde{P}}{\partial\phi_2} = \frac{\tilde{P}}{P^*}\left[P_1^* - P_2^* - \theta_2 X_{12}\left(1-\frac{\theta_1}{\phi_2}\right)\right] \tag{8.33}$$

$$C = \frac{\partial\tilde{T}}{\partial\phi_2} = \frac{\tilde{T}}{\tilde{P}}B + \frac{T}{P^*}\left(\frac{P_2^*}{T_2^*} - \frac{P_1^*}{T_1^*}\right) \tag{8.34}$$

These equations can be used to simulate the behaviour of various polymer mixtures.[5] For the simulations the contact entropy Q_{12} is the only adjustable parameter. X_{12} and Q_{12} are empirically interrelated:

$$Q_{12} \approx 2\times 10^{-3}\times X_{12}\ (\mathrm{K}^{-1}) \tag{8.35}$$

8.4 Parameters Influencing Miscibility

As can be seen from the above equation, X_{12} and Q_{12} are the parameters that control miscibility. In the absence of strong interactions such as hydrogen bonding, dipole-induced dipole or strong dipolar interactions, physical parameters or the equations of state parameters of the homopolymer become important. Clearly the equations of state parameters are also determined by polymer–polymer interactions but now the important factor is the relative balance between these interactions. Detailed theories have been produced which look in more detail at the effects of the various interactions.[6]

8.4.1 Molar Mass Dependence of Phase Diagrams[1]

One of the most important variables in a polymer system is the molar mass of the components. Figure 8.2 illustrates the phase diagrams for a variety of systems.

For strictly binary systems, appropriate differentiation of the free enthalpy of mixing leads to

$$\frac{\Delta\mu_1/RT}{m_1} = \frac{\ln\phi_1}{m_1} + \frac{1}{m_1} - \frac{\phi_1}{m_1} - \frac{\phi_2}{m_2} + \left(X_{12} - \phi_1\frac{\partial X_{12}}{\partial\phi_2}\right)\phi_2^2 \tag{8.36}$$

$$\frac{\Delta\mu_2/RT}{m_2} = \frac{\ln\phi_2}{m_2} + \frac{1}{m_2} - \frac{\phi_1}{m_1} - \frac{\phi_2}{m_2} + \left(X_{12} - \phi_2\frac{\partial X_{12}}{\partial\phi_1}\right)\phi_1^2 \tag{8.37}$$

For such systems the spinodal and critical conditions yield

$$\begin{aligned}\text{Spinodal}: \frac{1}{m_1\phi_1} + \frac{1}{m_2\phi_2} - 2X_{12} + 2(1-2\varphi_2)\frac{\partial X_{12}}{\partial\phi_2} \\ + \phi_2(1-\phi_2)\frac{\partial^2 X_{12}}{\partial\phi_2^2} = 0\end{aligned} \tag{8.38}$$

$$\begin{aligned}\text{Critical point}: \frac{1}{m_1\phi_1^2} - \frac{1}{m_2\phi_2^2} - \frac{6\partial X_{12}}{\partial\phi_2} + 3(1-2\phi_2)\frac{\partial^2 X_{12}}{\partial\phi_2^2} \\ + \phi_2(1-\phi_2)\frac{\partial^2 X_{12}}{\partial\phi_2^3} = 0\end{aligned} \tag{8.39}$$

The last three terms in eqn (8.38) reduce to $-2X_{12}$ and in eqn (8.39) to zero. If X_{12} does not depend on concentration then the critical points can be identified:

$$\phi_{2c} = \frac{m_1^{1/2}}{m_1^2 + m_2^2} \tag{8.40}$$

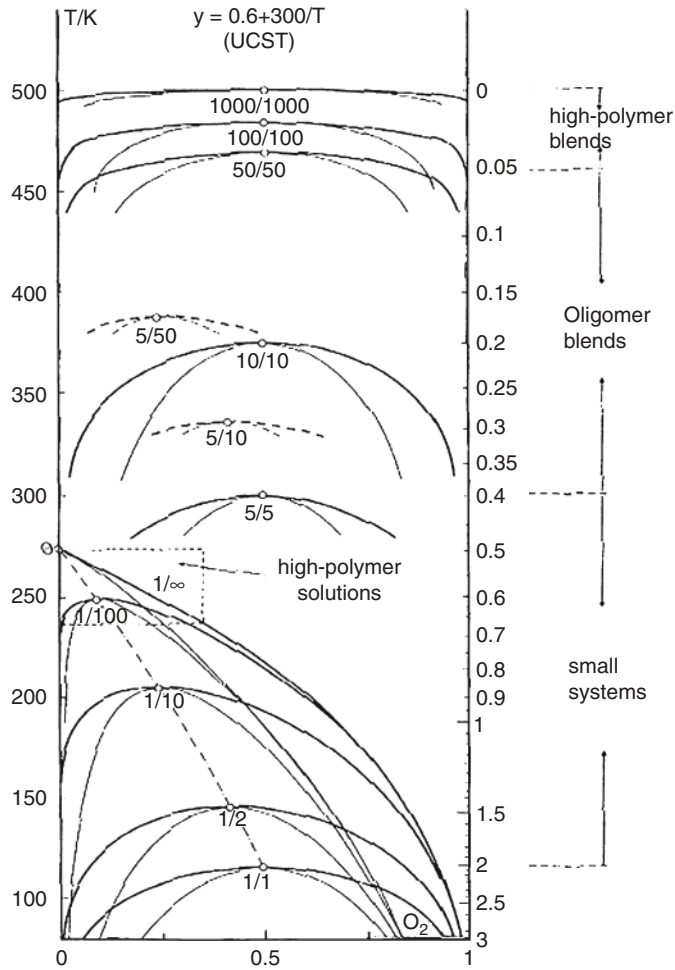

Figure 8.2 Binodals (heavy curves) as described by eqn (8.36) and (8.37) and spinodals (light curves) according to eqn (8.38) showing the effect of molar mass size (m_1/m_2). Open circles are critical points specified by eqn (8.40) and (8.41) and connected by the dash-dot curve.[1]

and

$$X_{12} = \frac{1}{2}(m_1^{1/2} + m_2^{1/2})^2 \tag{8.41}$$

For small molecules $m_1 = m_2 = 1$ but for high polymer solutions $m_1 = 1$, $m_2 > 1$, the critical value of X_{12} approaches $\frac{1}{2}$ for very large m_2 and the critical volume fraction of polymer becomes very small. When both m_1 and m_2 are very large X_{12c} is very small.

In general, as the molecular mass of the polymer is increased the minimum temperature at which phase separation starts is reduced. For an

80-fold increase in the molar mass the cloud point temperature reduces by about 60 °C.

8.4.2 Effect of Pressure on Miscibility

Mixtures with UCST behaviour usually become less miscible on applying pressure. Typically the pressure dependence is $\partial T/\partial P$ and is of the order of 0.01–0.05 °C atm^{-1}.

8.4.3 Addition of Block Copolymers

The addition of block copolymers to a binary polymer mixture can aid compatibilization of the components of the blend by reduction of the interfacial energy between the two phase separated domains. Copolymers can depress the build-up of the interfacial energy between the phases and/or make a favourable contribution to the entropy changes on mixing at the homogeneous/heterogeneous phase separation temperature with the result that phase separation is delayed.

8.4.4 Refinements of Theory

The theory presented above does not allow for lattice compressibility. This has been incorporated in the theory by modification of the interaction parameter X_{12} according to the theory of Sanchez and Lacombe:[7]

$$\chi_1 = R\rho_1\left\{X_{12} + \frac{1}{2}\psi^2\tilde{T}_1P_1^*\beta_1\right\} \tag{8.42}$$

where ψ is a dimensionless function and β_1 is the isothermal compressibility of component 1. The first term is the energetic contribution and the second one is an entropic contribution. According to this theory the following inequality must hold:

$$\frac{\partial(\Delta\mu_1/kT)}{\partial\phi_1} = \frac{1}{2}\left(\frac{1}{r_1\phi_1} + \frac{1}{r_2\phi_2}\right) - \tilde{\rho}\left(X_{12} + \frac{1}{2}\psi^2\tilde{T}P^*\beta\right) \succ 0 \tag{8.43}$$

where the first term is the combinatorial contribution, $\tilde{\rho}X_{12}$ is an energetic contribution and $\frac{1}{2}\tilde{\rho}\psi^2\tilde{T}P^*\beta$ is an entropic contribution from the equation of state. The combinatorial entropy makes a larger contribution on both sides of the spinodal curve. To relax this effect a correction entropy factor has been incorporated in the theory.

8.5 Kinetics of Phase Separation: The Spinodal Decomposition

The spinodal is the limit of metastability beyond which a homogeneous phase can no longer exist. Spinodal decomposition that differs from nucleation and growth is the mechanism by which a homogeneous blend starts to phase separate at the temperatures inside the spinodal region. The process is essentially the growth in the variation of concentration with time, a diffusion process driven by the free energy. The flux of material is against the concentration gradient resulting in a negative diffusion coefficient. In addition, impurities play a small or zero role in this mechanism in contrast to nucleation and growth.

At the early stage of spindonal decomposition infinitesimal fluctuations in the concentration start to grow, the phase sizes are very small and co-continuous/interconnected with decomposition occurring spontaneously.

A theoretical model based on a diffusion equation was developed by Cahn and Hilliard[8] and introduces a diffusion equation that relates the interdiffusional flux J of the two phases ($\tilde{J} = \tilde{J}_1 = -\tilde{J}_2$) to the gradient of chemical potential differences:

$$-\tilde{J} = M\Delta(\mu_1 - \mu_2) \tag{8.44}$$

where M is the diffusion mobility and is simply the ratio of diffusional flux to the local chemical potential. Thermodynamic considerations show that M is always positive.

The change in chemical potential for a heterogeneous mixture at the early stage of phase separation is given by

$$\mu_1 - \mu_2 = \frac{\partial \Delta G}{\partial \phi} - 3K\nabla^2\phi \tag{8.45}$$

where K is the gradient energy coefficient and is usually determined experimentally. However, it can be estimated independently from the dimensions of the polymers:

$$K = \frac{1}{6}\left[\frac{M_1}{M_{w1}\phi_1}R_{g1}^2 + \frac{M_2}{M_{w2}\phi_2}R_{g2}^2\right] \tag{8.46}$$

where M is the monomer mass, M_w is the molar mass of the polymer and R_g is the radius of gyration of the corresponding components. Substituting these results in eqn (8.44) gives

$$-\tilde{J} = M\frac{\partial^2 \Delta G}{\partial \phi^2}\nabla\phi - 2MK\nabla^2\phi \tag{8.47}$$

By taking the divergence of the above equation the general Cahn–Hilliard diffusion equation is obtained and this forms the basis of the interpretation of

the spinodal decomposition phenomena:

$$\frac{\partial \phi}{\partial t} = M \frac{\partial^2 \Delta G}{\partial \phi^2} \nabla^2 \phi - 2MK\nabla^4 \phi + \text{nonlinear terms} \tag{8.48}$$

The solution to eqn (8.47) is usually written in terms of the growth in amplitude of the concentration fluctuation with growth rate of $R(q)$ the scattering parameter which reflects phase separation:

$$R(q) = -M \frac{\partial^2 \Delta G}{\partial \phi^2} q^2 - 2MKq^4 \tag{8.49}$$

where q is the wavenumber, $q = (4\pi/\lambda) \sin(\theta/2)$, λ is the wavelength and θ is the scattering angle. From this equation it is apparent that the sign of $R(q)$ is governed by $\partial^2 \Delta G/\partial \phi^2$, since M, K and q are positive quantities. Thus $R(q)$ is negative in the homogeneous and metastable regions and only becomes positive within the spinodal phase region. Hence the phase separation should proceed spontaneously within the spinodal region at a scale governed by the values of q that yield a positive growth rate. The maximum growth rate appears at

$$q_m^2 = -\frac{1}{4K} \frac{\partial^2 \Delta G}{\partial \phi^2} \tag{8.50}$$

which corresponds to the most rapidly growing wavelength of

$$\lambda_m = \frac{2\pi}{q_m} \tag{8.51}$$

The scale of phase separation for polymer blends at the early stage of spinodal decomposition is very small and is of the order of a few hundreds or thousands of angstroms and is typical of the morphology found in many blended systems.

8.6 Specific Examples of Phase-Separated Systems

In the above discussion the theory has considered primarily the case of the mixing of two polymeric species. In Figure 8.1 it can be seen that similar behaviour is observed for a polymer dispersed in a solvent. Several technologically interesting examples of phase separation demonstrate the effect of transition from low molar mass to high molar mass on the phase behaviour of the mixture.

8.6.1 High-Impact Polystyrene[9]

Polystyrene is extensively used in a range of applications, such as car headlamp lenses, where its mechanical properties are important. Polystyrene has a T_g value of 100 °C and can withstand a reasonable impact. However, improvement of its impact properties is commercially desirable and requires incorporation of a

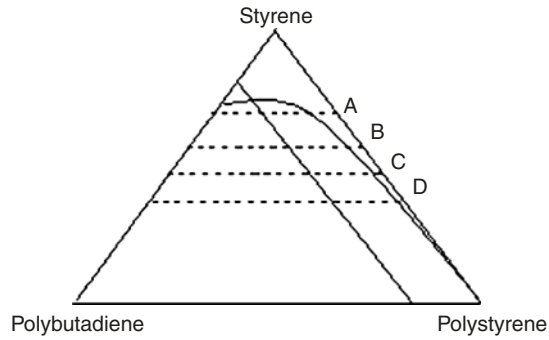

Figure 8.3 Ternary phase diagram for mixtures of styrene–polybutadiene–polystyrene.

mechanism for energy dissipation below T_g. High-impact polystyrene (HIPS) is a dispersion of polybutadiene within a matrix of polystyrene. The tertiary phase diagram for styrene–polybutadiene–polystyrene is shown in Figure 8.3. Polybutadiene will dissolve in styrene monomer to form a homogeneous single phase.

Initially droplets of a polystyrene-rich phase are formed within a polybutadiene-rich phase, designated in Figure 8.3 as tie line A. As the polymerization proceeds the ratio of the two phases will change until between B and C the volume fraction of the polystyrene-rich phase exceeds the volume fraction of the polybutadiene-rich phase and the mixture will phase invert so that the polystyrene phase becomes continuous (Figure 8.3).

The actual points of phase inversion depend on the viscosities of the phases and hence the molar mass of the polymer and on the rate of stirring within the reactor. The resultant morphology of a commercial material is shown in Figure 8.4. The polystyrene phases are trapped within the butadiene phase during the phase inversion and the complicated morphology formed is responsible for many of the advantageous physical properties of these blends.

8.6.2 Rubber Toughened Epoxy Resins[10]

Amine-cured epoxy resins are extensively used as structural matrices in composite manufacture and as such the improvement of their mechanical properties is very desirable. As in the case of polystyrene the addition of a rubber phase provides an energy dissipation mechanism below T_g and this increases the toughness of the overall material. Carboxy-terminated butadiene acrylonitrile (CTBN) is initially soluble in the reaction mixture of digylcidyl ether of bisphenol A (DGEBA) and the low-temperature cure system triethylenetetra-amine (TETA):

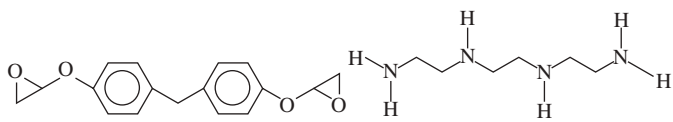

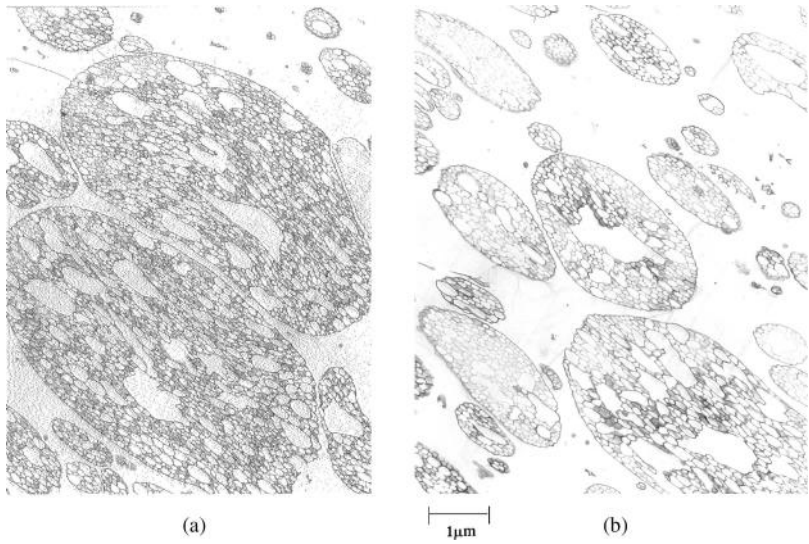

Figure 8.4 Transmission electron micrographs of HIPS showing the styrene dispersed within the butadiene phase that is in turn dispersed within the styrene phase. The isoprene phase is stained black.

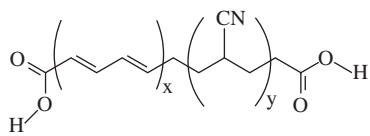

Carboxy-terminated butadiene acrylonitrile random copolymer (CTBN)

As in the case of the polystyrene system, increasing the molar mass of the epoxy resin polymer dispersed in the CTBN-rich phase will lead to phase separation.

Two chemically dissimilar polymers will naturally attempt to phase separate and the structure that is formed will reflect the way in which this process occurs and the driving forces associated with the process. Phase separation is used to achieve rubber toughening in thermoset resin systems. Low molar mass CTBN copolymer is soluble in the simple mixtures of monomers used to create amine-cured epoxy resins systems. However, as the molecular mass of the epoxy resin increases so the balance of entropy and enthalpy of mixing of these components changes and a driving force for phase separation is created.

Since the process of phase separation is both a kinetic and thermodynamic driven process the features that are created depend on the temperature and speed of the cure process. Rubber toughening is improved if the particles of the CTBN are small and evenly dispersed. The size of the particles formed depends on the temperature of the cure and the rate at which it occurs (Figure 8.5). In this example, contrast can be imparted to the sample by staining with osmium tetroxide. The osmium tetroxide can add to the double bonds of the butadiene. From the point of view of electron microscopy these regions have now a much

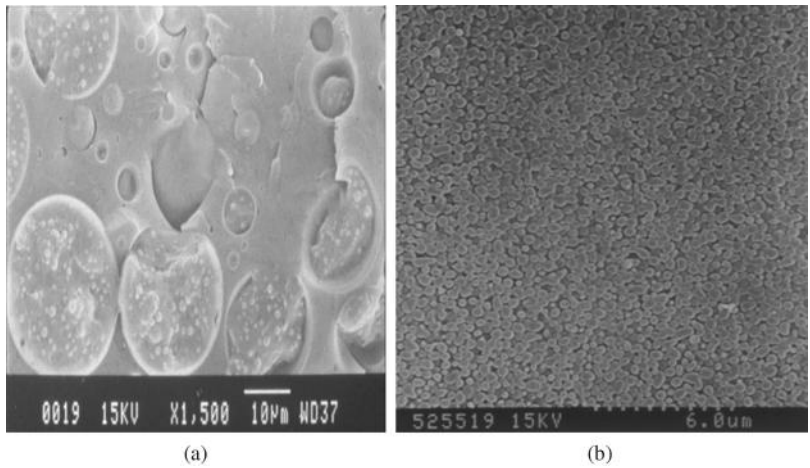

Figure 8.5 Electron micrographs of CTBN particles dispersed in an amine-cured epoxy resin. The morphology changes with the concentration of CTBN: (a) 3% CTBN; (b) 8% CTBN.

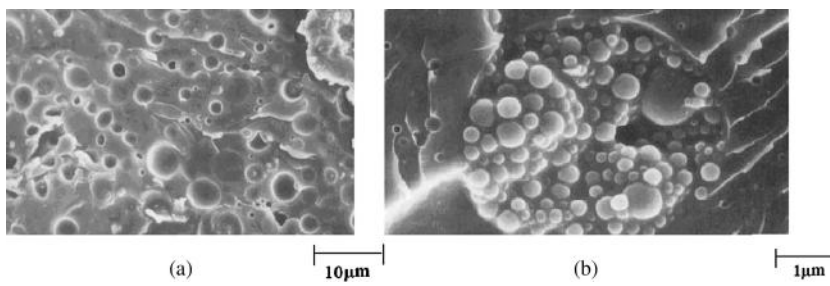

Figure 8.6 Morphology of TETA–DGEBA–CTBN systems: (a) low-resolution image showing the distribution of CTBN phases in the matrix; (b) enlargement of one of the CTBN phases showing the included epoxy nodules within the CTBN phase.

greater electron scattering efficiency than they had previously and contrast with the surrounding unstained areas of the epoxy resin.

Further increase in the concentration of the epoxy resin polymer will lead to a phase inversion within the CTBN phase. The nodules in the scanning electron microscopy images are of the phase separated epoxy phase (Figure 8.6). This behaviour has striking similarities to the HIPS system and the phase diagrams for this relatively polar system are strikingly similar to those of HIPS.

8.6.3 Thermoplastic Toughened Epoxy Resins

For structural application epoxy resins are cured at high temperatures and use an aromatic amine hardener rather than the aliphatic compounds indicated

above. A typical aerospace resin uses 4,4′-diaminodiphenylsulfone (DDS) together with DGEBA and a thermoplastic, poly(ether sulfone) (PES), as the toughening agent:[11]

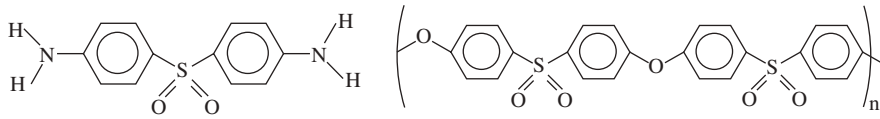

4,4'-diaminodiphenylsulfone (DDS) poly(ether sulfone) (PES)

As with the other examples discussed above, the PES is initially soluble in the mixture of DDS and DGEBA forming a homogeneous solution. As the cure process proceeds phase separation occurs and, depending on the concentration of the PES, the dominant morphology changes.[12] Between 0 and 2.5% of PES a homogeneous material is obtained. Above this concentration a particulate morphology is observed, with PES being the dominant component of the particulate phase. At approximately 22.5% the morphology is of a co-continuous structure and this is observed up to about 30%. Above 30% of PES in the system phase inversion occurs and the continuous matrix is now PES. These changes are illustrated in the electron micrographs in Figure 8.7.

In all the above examples the mechanical property enhancement is a consequence of spinodal decomposition of an initially homogeneous mixture to form a co-continuous phase separated structure.

8.6.4 Epoxy Resins

The synthesis of epoxy resins involves an addition process and usually involves the reaction of a primary aromatic or aliphatic amine with a di- or higher function epoxy compound. The initial reaction will create a linear molecule that contains secondary amine functions. These secondary amine functions are less reactive than the primary amines and the result of the initial reaction is to grow

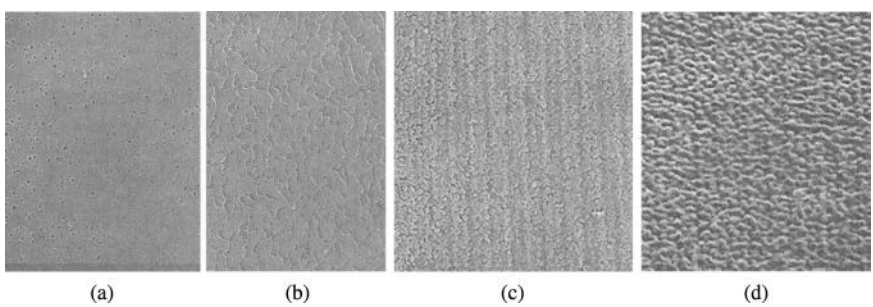

Figure 8.7 Electron micrographs showing the effects of an increase in PES concentration on the phase structure of an amine-cured epoxy resin: (a) 10% PES, (b) 20% PES, (c) 30% PES and (d) 35% PES.

linear polymers. As the reaction proceeds, the possibility of the creation of branched chain structures and ultimately cyclic ring structures increases:

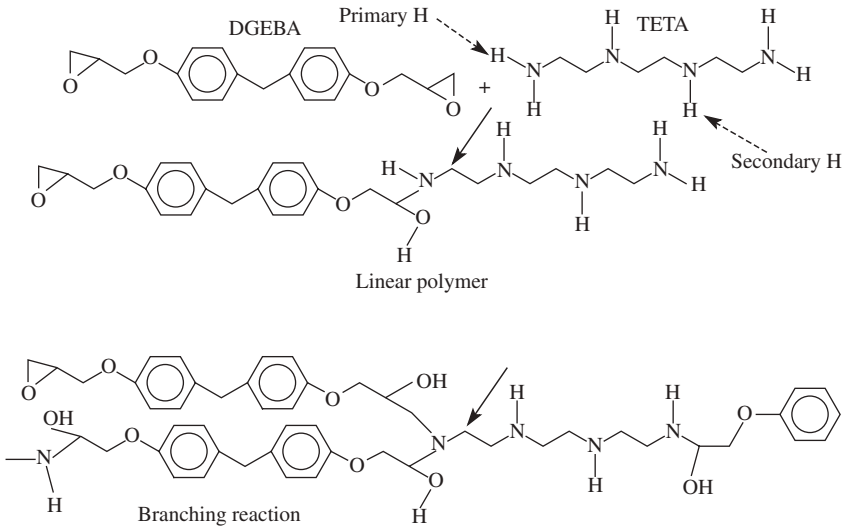

The final thermoset system is ideally a three-dimensional linked cyclic structure which extends through all space. However, in general, this process is never completed because not all the reactive functions can be consumed. In certain areas the formation of cyclic structures can be completed at an early stage in the reaction and these entities are now thermodynamically less compatible than the linear polymers with the monomers. As a consequence these crosslinked entities have higher values of T_g than the less highly crosslinked matrix in which they are dispersed. There is some evidence that these entities can phase separate during the course of the reaction and will influence the physical properties of the matrix that is formed. For instance when water enters the epoxy resin matrix it can plasticize the more open regions lowering T_g by about 10 °C for every 1% of water absorbed; however, these more highly crosslinked regions are less susceptible to moisture uptake and their T_g is often hardly depressed by exposure to water.

8.7 Block Copolymers: Polystyrene-*block*-Polybutadiene-*block*-Polystyrene (SBS) Block Copolymer

In the search for new materials, the idea of block copolymers emerged. Block copolymers are materials produced by the careful control of the synthesis a polymer and contain regular sequences of more than one type of monomer. In 1965, Shell brought to the market a number of polystyrene-*block*-polybutadiene-*block*-polystyrene and polystyrene-*block*-polyisoprene-*block*-polystyrene

materials. These materials show high strength and have a rubber elasticity that is comparable to that of rubber. This system has been extensively studied and is reviewed by Price and co-workers.[13] The behaviour reported for this system is typical of that found for all block copolymers, but can depend on the thermal history of the sample.

8.7.1 General Characteristics

The two polymers, polystyrene and polybutadiene, are immiscible (Figure 8.8). This has already been illustrated in the case of HIPS. Thermodynamically the blocks of the polymer will be incompatible and will attempt to phase separate.

Electron microscopy of stained samples of SBS copolymers (Figure 8.10) has shown that phase separation occurs in a controlled manner and produces highly regular structures in the solid state. Depending on the length of the block, typical values of m_1 and m_2 being of the order of 2000–3000 with n having a value of the order of 1000, different physical characteristics are observed. Polymers have also been produced in which the ratio of m_1 to m_2 is ~ 1 but varied in relation to n give differences in the morphology. Figure 8.9 represents these differences schematically for an AB or an ABA block copolymer system. As the concentration of the component A in the AB block is varied so the morphology changes.

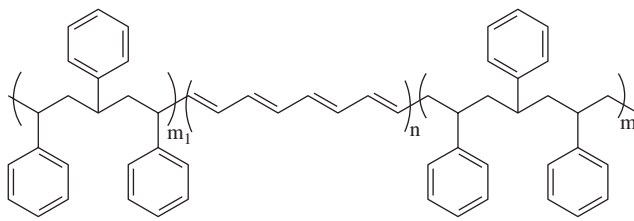

Figure 8.8 The idealized structure of the polystyrene-*block*-polybutadiene-*block*-polystyrene block copolymer; m_1 and m_2 denote the number of monomers in the styrene block and n denotes the number of monomers in the butadiene block.

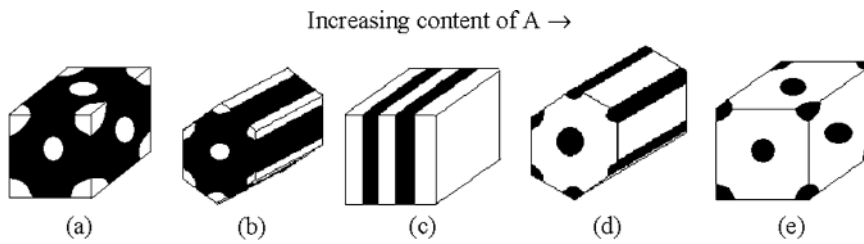

Figure 8.9 Effect of composition on block copolymer morphology: (a) spheres of A in matrix of B; (b) cylinders of A in matrix of B; (c) alternating A and B lamellae; (d) cylinders of B in matrix of A; (e) spheres of B in matrix of A.[13]

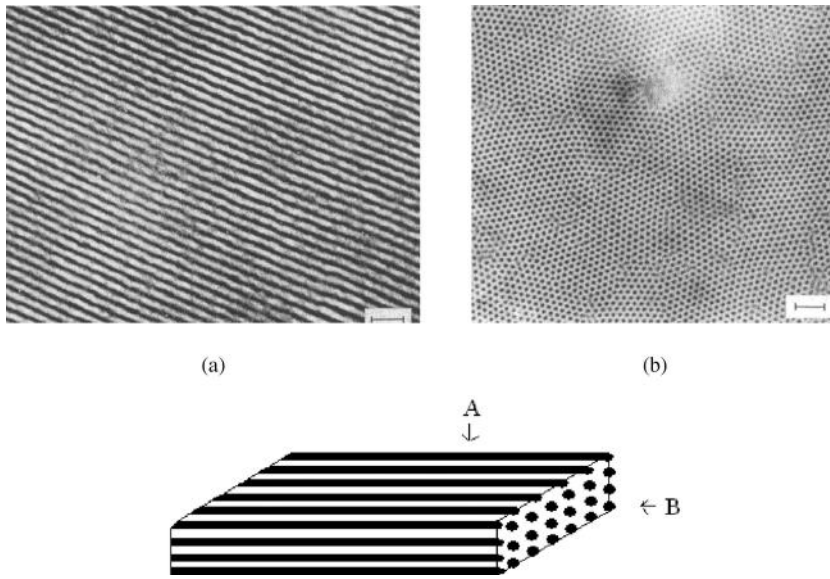

Figure 8.10 Osmium tetroxide stained electron micrographs of polystyrene-*block*-polybutadiene-*block*-polystyrene block copolymer produced by extrusion. (a) Micrograph demonstrating the orientation of the styrene cylinders in the direction of the extrusion (direction A in the schematic) and (b) shows a close-packed structure transverse to the extrusion direction (direction B in the schematic). Scale bar = 1 μm.

In practice, it is found that the degree of regularity of the domain structure depends very much on the physical treatment to which a sample has been subjected (Figure 8.10). Imposition of an external stress, as in the case of extrusion of the polymer through a die, will induce alignment of the phase-separating morphology and create the type of structures shown in Figure 8.10. The size of the features observed in the electron micrographs is dictated by the molar mass of the blocks in the polymer chain. The radius of the cylinders is determined by the radius of gyration of the blocks in the copolymer. The perfection of the morphological structure will depend on a combination of thermodynamic and kinetic factors. The thermodynamics will drive the system to phase separation and the kinetics will control the rate at which the phase separation is achieved. Similar structures are observed in diblock copolymers. Hence SBS diblock copolymer will exhibit a similar morphology but its mechanical characteristics are very different.

In the case of the SBS block copolymer the matrix structure is pinned by the styrene domains and whilst mobility is introduced once T_g of the butadiene phase has been exceeded, the material will not flow until the temperature has been raised above T_g of polystyrene. In contrast, whilst the low-temperature mechanical characteristics are similar with the material exhibiting elastic properties once T_g has been reached, the subsequent characteristics are less predictable since flow is possible below T_g of the polystyrene phase that is now unable to

anchor the material. Clearly there is an interface between the domains and there has been much discussion as to the thickness of the interfacial regions.

The most important factor deciding the type of equilibrium domain structure adopted by a system is the weight fraction of the components. The molar mass appears to play a secondary role in this respect, but strongly influences the location of the boundary defining the transition from homogeneous to microphase separated states. For SBS the body-centred cubic (bcc) polystyrene spheres are stable up to approximately 20 wt%, hexagonally packed polystyrene cylinders between approximately 20 and 40%, lamellae from 40 to 60%, polybutadeine cylinders from 64 to 82% and bcc polybutadiene spheres above 84%. Between 82 and 84% an orthorhombic structure has been reported which may be a metastable form. The phase diagram does, however, show some molar mass dependence, as shown in Figure 8.11.

The microdomain size D_i and lattice repeat distance d of periodically organized microdomains have the following approximate molecular mass dependence:

$$D_i \sim (M_i)_n^{2/3}; \quad d \sim (M)_n^{2/3} \tag{8.52}$$

where $(M_i)_n$ and $(M)_n$ are the number average molar masses of the blocks forming the domains and the overall number average molar mass of the copolymers, respectively. Because of the way block copolymers are prepared their molar mass distribution is often very narrow, typically 1.01.

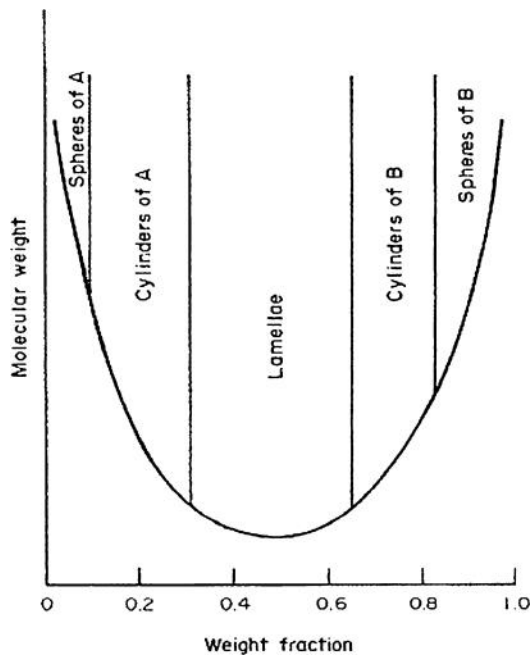

Figure 8.11 Phase diagram for the geometry, stability and microdomains of an AB-type block copolymer.[13]

8.7.2 Thickness of the Domain Interface

The thickness of the interfacial region is donated by δ and the phase is assumed to be strongly segregated so that $\delta \ll D_A, D_B$ (Figure 8.12). Away from these interfacial regions the domains consist either of pure A or pure B at the density of the homopolymer melt, $\rho_{0,A}$ and $\rho_{0,B}$ respectively.

The enthalpy of mixing ΔH_{mix} may be estimated using

$$\Delta H_{mix} = \gamma\xi - V\phi_A\phi_B\chi_{AB}kT \tag{8.53}$$

where ξ is the total surface area of the domains, γ is the surface tension between the phases, V is the total volume of the system, ϕ_A and ϕ_B are the volume fractions of A and B, respectively, and χ_{AB} is the Flory–Huggins interaction parameter for the system. The second term, which really drives the transition so that unfavourable high-energy A–B contacts are reduced, gives the enthalpy change on going from a randomly mixed state to the domains assuming no volume change, whilst the first term is the surface term. From space filling considerations we have

$$\xi D_A\rho_{0,A} = \xi D_B\rho_{0,B} = N_P \tag{8.54}$$

where N_P is the total number of copolymer chains. Hence

$$\Delta H_{mix} = \gamma N_P(D_A\rho_{0,A})^{-1} - V\phi_A\phi_B\chi_{AB}kT \tag{8.55}$$

and γ depends on the interactions between the blocks in the interfacial region and may be estimated for example in terms of χ_{AB} and δ. The entropy of mixing ΔS_j arises from the entropy change in placing the A–B junctions within an interfacial volume (V_j) and is estimated as

$$\Delta S_j = N_P k \ln\left(\frac{V_j}{V}\right) \approx N_P k \ln\left(\frac{\delta_{0,A}}{\left[D_A(\rho_{0,A} + \rho_{0,B})\right]}\right) \tag{8.56}$$

Finally, $\Delta S_{conformation}$ arises from the constraints that the blocks of the copolymer are restricted to domains. Because chains in the polymer melt behave as if they were ideal, *i.e.* as if there were no excluded volume effects, then it is frequently argued that Gaussian statistics should be applied to these domains of pure A and B and provided the inequality $L_k N_k^{1/2} < D_k < L_k N_k$ holds good

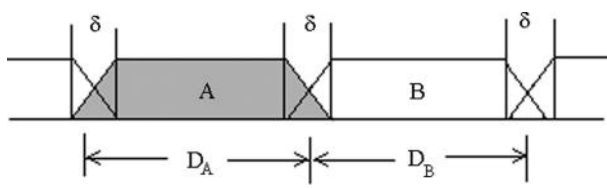

Figure 8.12 Density distribution of A and B segments in a block copolymer exhibiting microphase separation.

(k represents A or B) this leads to the result

$$\Delta S_{\text{conformation}} = k_A D_A^2 (N_A L_A^2)^{-1} + k_B D_B^2 (N_B L_B^2)^{-1} \tag{8.57}$$

where k_A and k_B are constants which may be estimated from the solution of the equation of motion for a random flight chain contained within the domain. If the above results are combined together the scaling law is obtained:

$$D_A \sim (N_A + N_B)^{2/3} \tag{8.58}$$

Meier[16] has estimated the thickness of the boundary layer to be given by

$$\gamma = \frac{kT\chi_{AB}\delta}{2} \tag{8.59}$$

There has been considerable interest in the estimation of the interfacial thickness but experiment has shown it to be of the order of a few monomer units.

8.8 Polyurethanes[14,15]

Polyurethanes are a very important class of materials that are readily synthesized by the reaction of an isocyanate with either a hydroxyl-containing polyester or polyether to form a polyurethane or reaction with an amine to form a urea. The urethane containing one NH and a carbonyl per bond has the capability of forming stable hydrogen bonds and in a typical chain-extended polyurethane phase separation is promoted to give a structure shown schematically in Figure 8.13. The 'rooftop' structure of the MDI promotes favourable packing and this is further stabilized by the π–π interactions between neighbouring phenyl groups and the favourable alignment of the urethane groups to achieve hydrogen bonding. This 'hard' block structure has a melting point of approximately 158 °C.

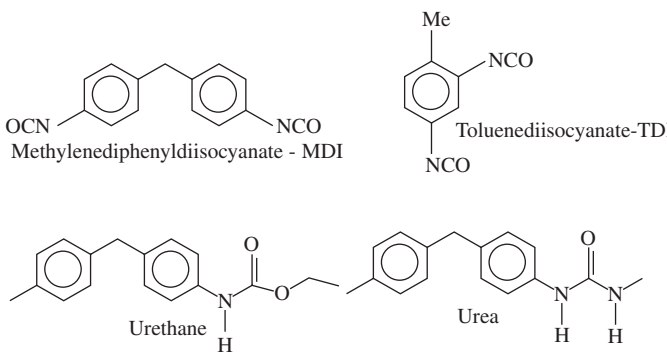

The urethane linkages can also hydrogen bond to the polyester and hence, unlike the SBS block copolymers, the interface between the hard block and the 'soft' predominantly ester or ether phase is diffuse rather than being sharp. The

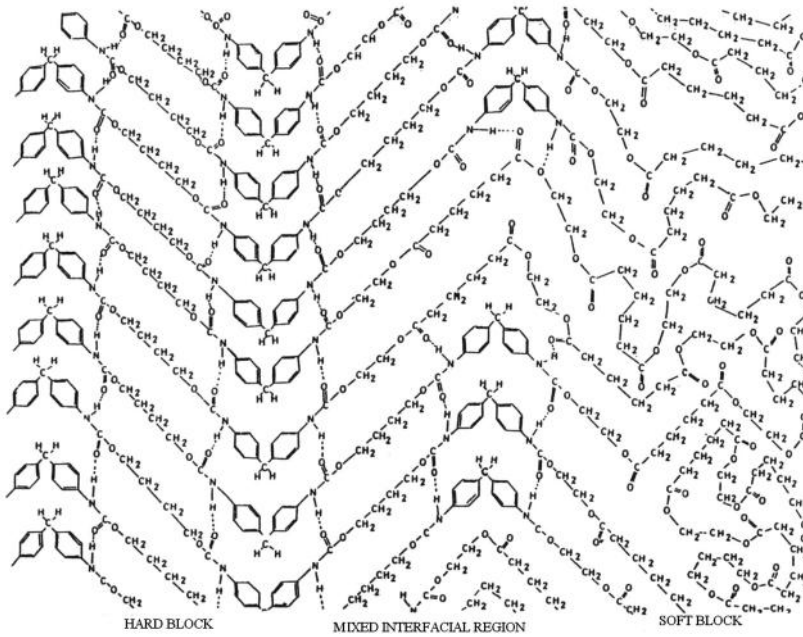

Figure 8.13 Schematic of the structure of a polyurethane.

ester or ether phases have values of T_g which are in the range $-20\,^{\circ}C$ to $20\,^{\circ}C$ depending on molar mass. This 'soft' phase imparts flexibility to the material and allows it to develop rubbery characteristics. Polyurethanes are extensively used in footwear and other applications where flexibility combined with structural integrity is required.

Evidence for phase separation can be obtained from a variety of different methods including dynamic mechanical thermal analysis; however, microscopy does not give clear images in the way that is observed for SBS.

There is current interest in the use of block copolymers to help create structures that have potential sensor applications,[17] e.g. block copolymers of polystyrene–poly(methyl methacrylate) (PS-b-PMMA). The nature of the organization that is created in thin films is influenced by the factors influencing phase separation of the polymers and very importantly the surface energy of the substrate on which they are deposited (Figure 8.14). If a substrate is patterned and then certain areas chemically modified, a substrate is created with variation in the surface energy across the surface. This is discussed in more detail in Chapter 9. The differences in surface energy will influence the morphology created.

On the left of Figure 8.14b, the surface is chemically homogeneous and the lamellae form a fingerprint morphology that lacks long-range order. On the right the surface is chemically stripped with a periodicity L_s that matches the block copolymer periodicity L_o and induces the lamellae to form perfectly ordered structures over large areas, similar to that observed for SBS

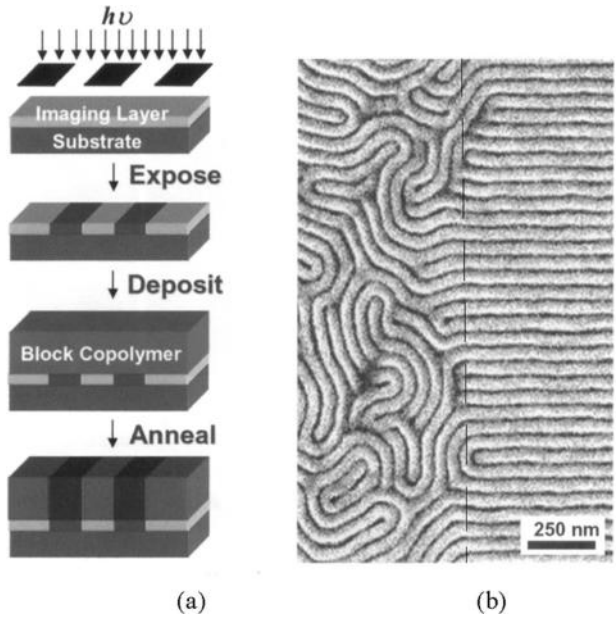

Figure 8.14 The substrate is patterned before the block copolymer is deposited (a). The resulting structure is shown in (b) and illustrates the effects of differences in surface energy on the morphology created. The dashed line indicates the boundary between the modified and unmodified areas.[17]

copolymers discussed above. It is possible using these patterns to deposit various inorganic materials and create functional ordered structures which can be used to fabricate sensors. The creation of these devices is only possible because of the principles of thermodynamics which govern the formation of these morphologies.

Recommended Reading

R.A. Brown, A.J. Masters, C. Price and X.F. Yuan, in *Comprehensive Polymer Science*, ed. G. Allan, Pergamon, 1989, vol. 2, p. 155.
S. Rostami, in *Multicomponent Polymer Systems*, ed. I.S. Miles and S. Rostami, Longman Scientific & Technical, Harlow, UK, 1992, p. 63.

References

1. R. Koningveld, W.H. Stockmayer and E. Neis, *Polymer Phase Diagrams: A Textbook*, Oxford University Press, 2001.
2. J.S. Rowlinson and F.L. Swinton, *Liquid and Liquid Mixtures*, Butterworths, 1982.

3. S. Rostami, in *Multicomponent Polymer Systems*, ed. I.S. Miles and S. Rostami, Longman Scientific & Technical, Harlow, UK, 1992, p. 63.
4. A. Bondi, *J. Phys. Chem.*, 1964, **68**, 441.
5. S. Rostami and D.J. Walsh, *Macromolecules*, 1984, **17**, 315.
6. S.I. Kuchanov and S.V. Panyukov, in *Comprehensive Polymer Science, Second Supplement*, ed. G. Allan, Pergamon, 1996, p. 441.
7. I.C. Sanchez and R.H. Lacombe, *Macromolecules*, 1978, **11**, 1145.
8. W.G. Cahn and J.E. Hilliard, *J. Chem. Phys.*, 1958, **28**, 258.
9. D.J. Walsh, in *Comprehensive Polymer Science*, ed. G. Allan, Pergamon, 1989, vol. 2, p. 135.
10. C. Delides, D. Hayward, R.A. Pethrick and A.S. Vatalis, *J. Appl. Polym. Sci.*, 1993, **47**, 2037.
11. A.J. MacKinnon, S.D. Jenkins, P.T. McGrail and R.A. Pethrick, *Macromolecules*, 1992, **25**, 3492.
12. A.J. MacKinnon, S.D. Jenkins, P.T. McGrail and R.A. Pethrick, *Polymer*, 1993, **34**, 3252.
13. R.A. Brown, A.J. Masters, C. Price and X.F. Yuan, in *Comprehensive Polymer Science*, ed. G. Allan, Pergamon, 1989, vol. 2, p. 155.
14. R.A. Pethrick and C. Delides, *Eur. Polym. J.*, 1981, **17**, 675.
15. R.A. Pethrick, C. Delides, A.V. Cunliffe and P.G. Klein, *Polymer*, 1981, **22**, 1205.
16. D.J. Meier, *J. Polym. Sci., Part C*, 1969, **26**, 81.
17. M.P. Stoykovich and P. F. Nealey, *Mater. Today*, 2006, **9**(9), 20–29.